Annu. Rev. Earth Planet. Sci. 2002. 30:207–35
DOI: 10.1146/annurev.earth.30.091201.140550

PETROLOGY OF SUBDUCTED SLABS

Stefano Poli[1] and Max W. Schmidt[2]
[1]*Università degli Studi di Milano, Dipartimento di Scienze della Terra, Via Botticelli 23, 20133 Milano, Italy; e-mail: Stefano.Poli@unimi.it*
[2]*Institute for Mineralogy and Petrology, ETH-Zürich, 8092 Zürich, Switzerland; e-mail: Max.Schmidt@erdw.ethz.ch*

Key Words phase diagram, experiment, peridotite, basalt, sediment

■ **Abstract** The subducted lithosphere is composed of a complex pattern of chemical systems that undergo continuous and discontinuous phase transformation, through pressure and temperature variations. Volatile recycling plays a major geodynamic role in triggering mass transfer, melting, and volcanism. Although buoyancy forces are controlled by modal amounts of the most abundant phases, usually volatile-free, petrogenesis and chemical differentiation are controlled by the occurrence of minor phases, most of them volatile-bearing. Devolatilization of the subducted lithosphere is a continuous process distributed over more than 300 km of the slab-mantle interface. Melting of the subducted crust, if any, along sufficiently hot P-T paths, is governed by fluid-absent reactions, even though the difference between fluid and melt vanishes at pressures above the second critical end point. The density distribution at a depth of 660 km suggests episodic penetration in space and time of subducted slabs into the lower mantle and sinking down to the D″ region at the core-mantle boundary.

INTRODUCTION[1]

Subduction zones are the loci of most paroxistic phenomena on the Earth's surface, including explosive volcanic activity, high-magnitude earthquakes, fast morphological evolution, and deeply contrasting thermal fields. The evolution of a subduction zone system is intimately related to petrological reactions in the

[1]**Mineral Abbreviations** A: phase A; ab: albite; amp: amphibole; an: anorthite; and: andalusite; atg: antigorite; bio: biotite; br: brucite; Ca-per: Ca-perovskite; CAS: unknown CaO-, Al_2O_3-, SiO_2-rich phase; cc: calcite; cen: clinoenstatite; chl: chlorite; cld: chloritoid; coe: coesite; cpx: clinopyroxene; di: diopside; dol: dolomite; en: enstatite; epi: epidote; fo: forsterite; gar: garnet; gr: grossular; ilm: $MgSiO_3$ ilmenite; k-holl: K-hollandite; ky: kyanite; law: lawsonite; mag: magnesite; maj: majorite; Mg-per: Mg-perovskite; mus: muscovite; mw: magnesiowüstite; oen: orthoenstatite; ol: olivine; opx: orthopyroxene; or: orthoclase; p: periclase; par: paragonite; plg: plagioclase; py: pyrope; q: quartz; rw: ringwoodite; sill: sillimanite; sp: spinel; st: stishovite; sta: staurolite; ta: talc; wa: wadeite; wd: wadsleyite; wo: wollastonite; zo: zoisite; 10Å: 10Å-phase.

subducting slab that control buoyancy forces, drive slab pull, and account for volatile transport and release. The critical role of "fluids" in subduction zone environments has been addressed since the early 1970s, when the plate tectonic framework, modern geochemistry, and high-pressure experimental petrology provided a consistent indication of major processes occurring at convergent plate margins. Fluids promote mass transfer and energy release both in thermal and mechanical forms. Even though buoyancy forces are substantially controlled by fractions of most abundant phases, a number of chemical and rheological properties of subducted materials are controlled by minor amounts of key phases (Figure 1).

Thermomechanical models of the subducting slabs and of the overlaying mantle wedge consistently suggest that temperatures as low as 600–800°C might be encountered in the coldest "nose," down to depths on the order of 400 km (Kincaid & Sacks 1997, Davies & Stevenson 1992). Even though thermomechanical models largely differ on evolution with time, extent, and location of the coldest region (i.e., close to the top of the slab or a few tens of kilometers inside the slab), as well as on temperature distribution and evolution in the mantle wedge, all models agree that extreme temperature gradients occur across the slab-mantle interface. Therefore, a wide pressure-temperature-composition space has to be characterized to predict the evolution of subducting slabs.

1. SUBDUCTED MATERIALS: A SECTION THROUGH THE OCEANIC CRUST

In order to model physical and chemical properties of the subducted oceanic lithosphere, it is common practice to assume a very simplified lithologic section of the oceanic lithosphere that includes an upper layer of sediments, a layer of igneous rocks having a middle ocean ridge basalt (MORB) bulk composition, and a lower layer of depleted peridotites. However, modern ocean floors and ophiolites reveal large structural and chemical heterogeneities in the form of layers and pods that are expected to be maintained even under extreme strain rates if their dimension is in the order of tens of meters or higher. This is visible in eclogite-facies terrains of orogenic belts, where primary chemical and structural heterogeneities are responsible for distinct mineral assemblages and rheological behavior. Such variations are the result of a complex pattern of sedimentary, igneous, and metamorphic processes occurring at mid-ocean ridges, on the seafloor, and at trenches.

1.1. The Sedimentary Contribution

Thickness and composition of subducted sediments (see the Supplemental Materials link in the online version of this chapter or at http://www.annualreviews.org/) are functions of the sedimentary processes occurring on the ocean floor and in the forearc region as well as functions of the tectonic processes near the toe of the rigid rock framework of the overriding plate. Factors substantially reducing the volume of subducted sedimentary material include sediment compaction and fluid

expulsion in the trench region, sediment off-scraping and incorporation in accretionary prisms, underplating, and accretion to the core buttress of the overriding plate. Conversely, the occurrence of subduction erosion of the continental margin may enhance the amount of sialic material involved in subduction (von Huene & Scholl 1991).

Relative proportions of these phenomena are largely dependent upon relative plate motions and the resulting geometry of the wedge, and on processes occurring on the overriding continent. Even though there is no rule of thumb to assess the amount of subcrustally subducted sediments, the average thickness is commonly in the order of only a few hundreds of meters. However, they can be nearly absent (e.g., Tonga) or kilometers thick (e.g., Cascades). Furthermore, even though global estimates of subducted sediments reveal the dominance of terrigenous material (70–80 wt% on a fluid free basis) over carbonates (10–15 wt%) and opal (10–15 wt%) (Rea & Ruff 1996, Plank & Langmuir 1998), large variations are possible (Figure 2): Mid- and South America subduction zones involve large volumes of carbonate sediments, whereas subductions in the Northern Pacific are substantially carbonate free but opal rich.

Sediment chemistry is substantially controlled by sedimentological parameters such as the relative proportion of biogenic versus detrital components, the source of detrital material, and the sedimentation rate (Plank & Langmuir 1998). Strongly peraluminous material ($Al_2O_3 \approx 20$–25 wt%) is found only in continental shales and therefore is part of the terrigenous contribution. Mg/(Mg + Fe) in most

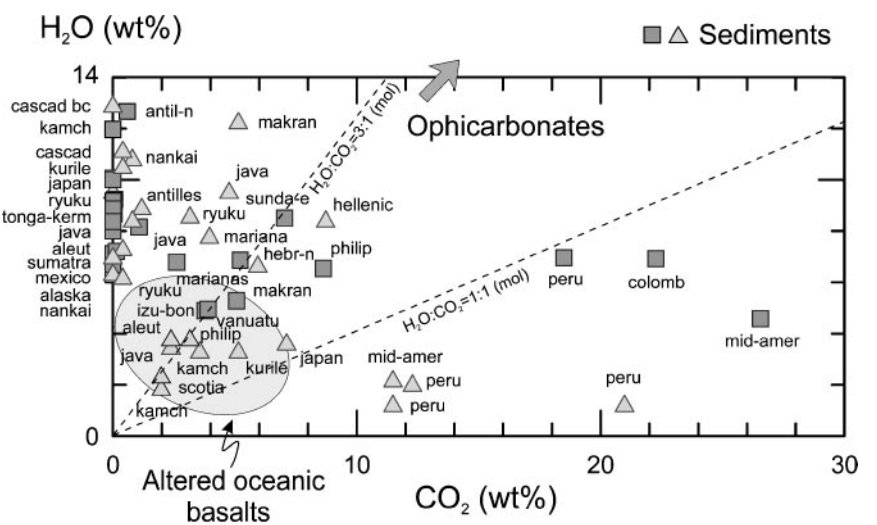

Figure 2 Estimates of the amount of H_2O in hydrates and CO_2 in carbonates in crustal columns being subducted. From Plank & Langmuir (1998) (*squares*) and Rea & Ruff (1996) (*triangles*). The shaded field represents altered MORB (Staudigel et al. 1996). Ophicarbonates after the data in Sciuto & Ottonello (1995) and Bonatti et al. (1974).

sediments approaches a value of 0.5; compositions outside the range of 0.4–0.6 are unusual.

1.2. Igneous Complexes in the Oceanic Crust

The oceanic lithosphere of mafic and ultramafic composition is the result of a complex sequence of igneous and metamorphic processes, usually accompanied by a history of both brittle and ductile deformation.

When fast spreading rates prevail (>100 mm $\cdot$ a^{-1}), e.g., in the East Pacific Rise since the Cretaceous, a layered sequence forms (Figure 3) including a mafic volcanic complex (pillows); a sheeted dike complex; an upper gabbroic complex of chemical composition very similar to the sheeted dike complex; highly differentiated gabbros (Mg-gabbros and troctolites, Fe-Ti gabbros) with layered, cumulitic textures; impregnated plagioclase-dunites; and depleted harzburgites with metamorphic tectonic fabric (Boudier & Nicolas 1995 and references therein). Whole-rock chemistry in cumulitic gabbros is dominated by the relative proportions of olivine and plagioclase (see the Supplemental Materials link in the online version of this chapter or at http://www.annualreviews.org/). Al_2O_3, MgO or CaO may exceed 20 wt% in Mg-gabbros and troctolites (Hekinian et al. 1993, Constantin 1999).

A completely different lithospheric section forms at slow-spreading centers (<50 mm $\cdot$ a^{-1}). An increasing amount of morphological, structural, and petrological data on the Atlantic, Arctic, and Indian oceans has revealed that serpentinized mantle does occur along slow-spreading ridges (Cannat 1993, Gente et al. 1995). Slow-spreading centers display deep rift valleys and a strongly fragmented lithosphere as a result of active extensional tectonics and amagmatic spreading. Deep normal faulting, down to 6–8 km depth, and crustal tilting are responsible for exposing lower crustal sequences and mantle peridotites at the ocean floor; gabbros are expected to form in small (a few kilometers wide) dike-like bodies, forming ephemeral magmatic chambers (Figure 3).

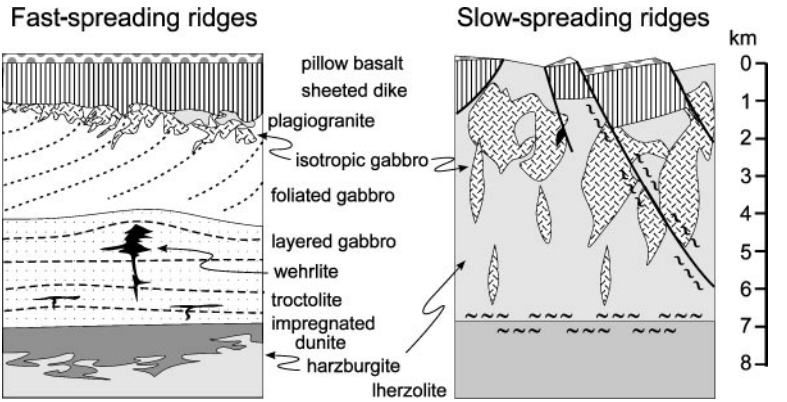

Figure 3 Schematic sections of the crust in fast- and slow-spreading oceans.

1.3. The Effects of Ocean Floor Metamorphism

Depth and intensity of hydrothermal alteration of the oceanic crust are a function of both thermal regimes and tectonic fragmentation of the lithospheric section (Alt 1995). Therefore, the presence of deep axial valleys, intense faulting, and block tilting is responsible for extensive metamorphism of the entire crustal section of slow-spreading oceans. On the contrary, continuous igneous events provide the heat to supply a vigorous hydrothermal circulation at fast-spreading ridges. Most abyssal peridotites show extensive serpentinization (50% to 90%) coupled to a MgO loss by 5–10 wt%, and SiO_2 enrichment higher than 5 wt%. This phenomenon has been ascribed to the incongruent dissolution of olivine and/or brucite (Snow & Dick 1995). During the off-axis passive circulation, the main alteration process to depths of a few hundreds of meters is the precipitation of carbonates (both calcite and aragonite) in cracks and voids.

The net fluxes between seawater and oceanic crust are relatively low (Staudigel et al. 1996). Most processes imply an internal element redistribution typically on a 10–100-m scale. Major addition of H_2O and CO_2 in the uppermost layer (Figure 2) and discontinuous but sometimes extensive hydration of the lower crustal sequence as well as of mantle peridotites are the most significant chemical variations. In extreme cases oceanic metamorphism may form amphiboles containing 3 wt% Cl (Magenheim et al. 1995) and serpentine (lizardite) with 0.36 wt% Cl (Scambelluri et al. 1997).

Last, but not least, ophicarbonates represent a peculiar rock type of oceanic environments. Ophicarbonates (see the Supplemental Materials link in the online version of this chapter or at http://www.annualreviews.org/) are dredged from fracture zones along the Mid-Atlantic ridge system (Bonatti et al. 1974), and they commonly occur in ophiolites where they may reach up to 100 m in thickness. Ophicarbonates consist of breccias of serpentinite fragments and micritic pelloids, cemented by a calcitic matrix, and have roughly equal proportions of hydrates and carbonates. Ultramafics pervasively altered from water-rock interactions may approach a chemical composition close to these breccias (Sciuto & Ottonello 1995). Despite their secondary importance in volume, the high amount of carbonates suggest a major role of ophicarbonates in the CO_2 cycle at convergent plate boundaries (Kerrick & Connolly 1998).

2. PHASE TRANSFORMATIONS ALONG SUBDUCTION PATHS: SOME PRINCIPLES

2.1. Fluid-Absent Versus Fluid-Present Conditions

The heterogeneous volatile distribution, which is an intrinsic feature of the altered oceanic crust, implies the presence or the absence of hydrates and/or carbonates, as well as the occurrence of both H_2O- and CO_2-saturated and H_2O-CO_2-undersaturated domains. The stability of a hydrate and/or a carbonate implies neither the presence of a free-fluid phase nor H_2O- and/or CO_2-saturation,

respectively. It is often suggested that a fluid should occur in shallow environments, whereas relatively "dry" conditions should affect high-pressure "eclogite-facies" rocks. This concept is based on the assumed identity of abundance of volatile components (mostly H_2O and CO_2) and abundance of fluids. However, as the appearance of a fluid is related to the thermodynamic definition of saturation, the relationships between the amount of volatiles and the presence of a fluid are not straightforward.

Simple model chemographies where multiple hydrates or carbonates are present [e.g., the system MgO-SiO_2-H_2O, Figure 4*a*,*b*; or CaO-MgO-SiO_2-CO_2, Figure 4*c*,*d*] reveal that a hydrate-bearing assemblage (anti-gorite + enstatite + forsterite, Figure 4*a*) or a carbonate bearing assemblage (dolomite + magnesite + enstatite, Figure 4*c*) does not require a free fluid to be stable and that hydrate- or carbonate-bearing reactions do not necessarily require H_2O or CO_2 as a reactant or as a reaction product. As an example, the reaction forsterite + talc = antigorite + enstatite (Figure 4*a*) may take place without consumption or release of H_2O; the reaction enstatite + dolomite = magnesite + diopside may take place without change in CO_2 (Figure 4*c*,*d*). Because low-temperature, low-pressure metamorphism promotes the formation of hydrous minerals that contain large amounts of H_2O (e.g., antigorite, talc, chlorite, lawsonite, etc.), the likelihood of H_2O-undersaturated assemblages and of H_2O-conserving reactions is maximized in such conditions. The attainment of H_2O-saturation, or conversely CO_2-saturation, i.e., the appearance of an aqueous or a carbonic fluid, is then controlled by the relative positions of P-T paths for the subducting slab, of H_2O or CO_2 saturation surfaces, and of chemical potential of H_2O or CO_2 (μ_{H_2O} and μ_{CO_2}) as buffered by hydrate- or carbonate-bearing assemblages in $G - P - T$ space.

In Figure 4*e* the breakdown reaction of antigorite is defined by the intersection of the thermodynamic surface of water (H_2O-saturation) with the light-blue surface, representing the chemical potential of H_2O buffered by the assemblage antigorite + enstatite + forsterite. A partially serpentinized peridotite from the ocean floor (which is the most probable case) shows an H_2O-undersaturated assemblage in Figure 4*a*. When such partially hydrated peridotite is involved in a prograde P-T path during subduction, the chemical potential of H_2O moves on the light-blue surface of Figure 4*e*. Like most dehydration reactions, i.e., reactions defined by the intersection of water surface with the surface where μ_{H_2O} is buffered by hydrates only, antigorite breakdown has a steep dP/dT slope and a prograde P-T path invariably leads to the release of an aqueous fluid.

Similarly, if we consider the evolution of magnesite + quartz, the appearance of a carbonic fluid is driven by the displacement of the chemical potential of CO_2 on the orange surface, where μ_{CO_2} is buffered by magnesite + quartz + enstatite, toward the thermodynamic surface of the carbonic fluid. However, as a result of the large $d\bar{G}/dP$ (i.e., equilibrium molar volume) for a pure CO_2 fluid, most decarbonation reactions have relatively "flat" dP/dT slopes, and P-T-μ paths progressively depart from saturation and therefore from fluid release. Even though there is no simple rule to predict if a system approaches or moves away from

fluid saturation, the general features of μ_{H_2O} and μ_{CO_2} shown in Figure 4 suggest that P-T paths for subducted slabs most likely lead to dehydration but not to decarbonation.

Following a similar line of reasoning, when both volatiles are present and saturation is obtained, the fluid is progressively H_2O enriched as pressure increases during subduction, i.e., a relatively carbonate-rich solid will coexist with a H_2O-rich fluid. This phenomenon has been shown theoretically by Kerrick & Connolly (1998) on ophicarbonate compositions and experimentally by Molina & Poli (2000) on basaltic compositions (see section 3.2).

2.2. Fluid Composition

Even though high-pressure, low-temperature fluids closely approach the H_2O-CO_2 join on a C-O-H diagram (Connolly & Cesare 1996) as a result of a progressive shift of the graphite boundary toward the H_2O end point, other minor species have an important role in the stability of the volatile-bearing phase. Oxygen fugacity, fO_2, exerts major control on the mutual stability of carbonates and graphite/diamond in a variety of mineral assemblages (Luth 1999).

Further complexity is introduced by the presence of dissolved silicates. Pioneering experimental work by Kennedy et al. (1962) and Nakamura & Kushiro (1974) revealed that fluids at high pressure may contain large amounts of dissolved solid matter. Conversely, melts, when present, dissolve large amounts of volatiles, mostly H_2O, potentially leading to the identity of fluid and melt phase at the so-called second critical end point. Boettcher & Wyllie (1969) thoroughly illustrated that the location in pressure and temperature space of this point is a function of the topology of the liquidus as well as of the vaporous surfaces. Therefore, in the simple system SiO_2-H_2O, the second critical end point is at only 1 GPa, 1100°C (Kennedy et al. 1962); in albite-H_2O and haplogranitic systems, it moves to ≈1.5 GPa (Bureau & Keppler, 1999); and in CaO-SiO_2-H_2O-CO_2, to 3.2 GPa, 500°C (Boettcher & Wyllie 1969); whereas in the ultramafic model system MgO-SiO_2-H_2O (MSH), the solidus terminates at ≈12 GPa, 1100°C (Stalder et al. 2000). In the system quartz + H_2O, silica dissolved in the fluid ranges from a few wt% at 500–700°C to a maximum of 12 wt% at 1 GPa, 900°C. In MSH at 6 GPa, the amount of silicate dissolved in the fluid does not exceed ≈10 wt% up to temperatures close to the solidus (≈1150°C). Experiments performed by Schneider & Eggler (1986) suggest quantities of solute from 3 wt% in an amphibole peridotite at 1.5–2.0 GPa, 750–900°C to 12–15 wt% in a phlogopite peridotite at 1.3–2.0 GPa, 1100°C. Addition of CO_2 to the fluid strongly depresses solubility of silicates by approximately one order of magnitude. As a whole, all of this experimental evidence may suggest that, for the relatively cold P-T paths typical for subducting slabs, the amount of solute in pure aqueous or carbonic fluids is relevant but relatively low to at least 3–4 GPa.

A somewhat different scenario may arise when chlorine is present in significant amounts (Brenan et al. 1995, Keppler 1996, Shmulovich et al. 2001). Even though

the effect of chlorine in high-pressure fluids is poorly explored, the possible development of highly saline fluids in subduction environments has been demonstrated by systematic studies on fluid inclusions in ultramafic and mafic-intermediate rocks (Scambelluri et al. 1997, Scambelluri & Philippot 2001). Saline fluids are also expected to originate from Cl-bearing minerals crystallized during oceanic metamorphism. Precipitation of a variety of solids in such inclusions suggests that the amount of solutes may reach 50% by weight in some cases.

2.3. Effect of Discontinuous Versus Continuous Reactions

There is a significant underevaluation of the consequences of continuous reactions on volatile release in complex natural systems. Phase transformations in subducting slabs are mostly interpreted on the basis of relatively simple model systems (e.g., MSH in ultramafic rocks). In such model systems, solid solutions are inhibited by the absence of proper chemical components; consequently, most reactions are discontinuous reactions. If a discontinuous reaction is a dehydration or a decarbonation reaction, it implies a focused release of fluid at unique P-T conditions (univariant equilibrium). However, natural complex systems are dominated by solid solutions with extremely large compositional fields, e.g., amphibole, chlorite, garnet, pyroxenes, micas, etc. As a result, even though the "critical" volatile-bearing phase does not show significant compositional variability, as is the case for lawsonite as an example, it may be that its breakdown reaction involves a number of solid solutions and is therefore continuous in character (see section 3.2). Consequently, in most natural systems devolatilization reactions in subducting slabs are continuous, and fluid release tends to be smeared out over a P-T range (or depth range) rather than focused in discrete flushes.

3. A SUMMARY OF PHASE RELATIONSHIPS IN SUBDUCTED MATERIALS

Current knowledge of high-pressure rocks is substantially based on experiments performed either at dry conditions or at volatile saturation. Nevertheless, in most cases, such experiments strongly constrain volatile undersaturated relationships, e.g., via chemographic and Schreinemakers' analyses.

3.1. Ultramafic Systems

Despite the extensive experimental work devoted to melting of pyrolitic and lherzolitic ultramafic rocks at both dry and wet conditions in hydrate- and/or carbonate-bearing assemblages, phase relationships in the subsolidus are still poorly explored, and mostly based either on systematic studies of simple model systems (MSH, MSH + Al_2O_3 − MASH; Ulmer & Trommsdorff 1999, Ohtani et al. 2000, Stalder & Ulmer 2001) or on reconnaissance experiments performed on bulk compositions approaching natural peridotites (Kawamoto et al. 1996, Fumagalli & Poli

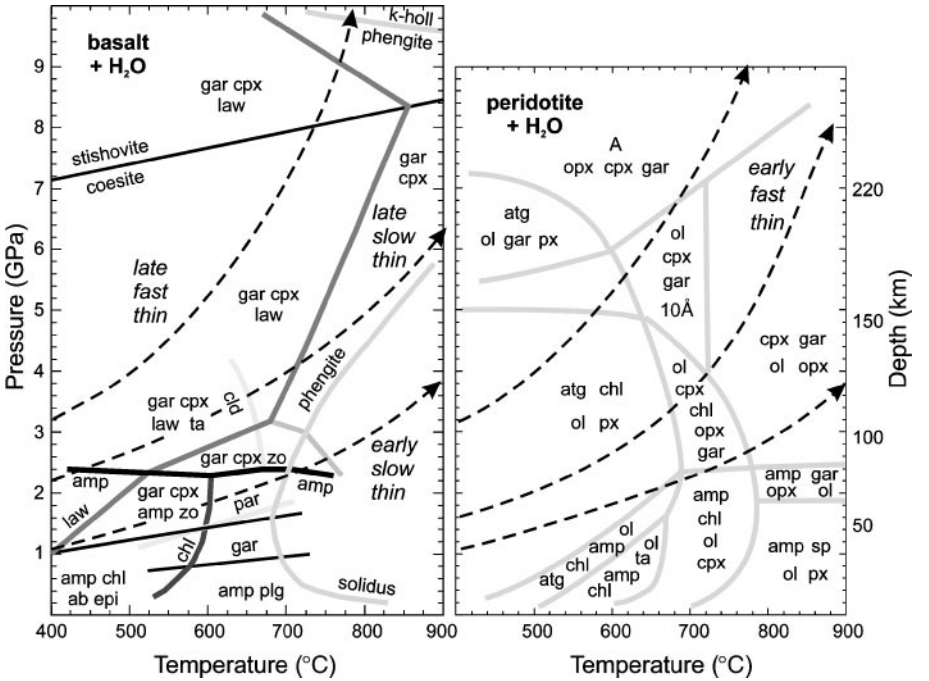

Figure 5 Schematic petrogenetic grid for tholeiitic basalt and lherzolite compositions at H_2O-saturated conditions, after Schmidt & Poli 1998, Ulmer & Trommsdorff 1999, Fumagalli 2000. Pressure-temperature conditions for (dis)appearance of hydrates are strongly controlled by whole-rock composition via continuous reactions, as shown in Figure 6. Dashed lines represent possible P-T paths for subducting slabs after Kincaid & Sacks 1997.

1999, Fumagalli 2000). A summary of H_2O-saturated phase relationships in ultramafic rocks is reported in Figure 5. Low temperature assemblages are dominated, in a pressure interval of more than 6 GPa, by the occurrence of antigorite (Ulmer & Trommsdorff 1999; Wunder 1998). If sufficient aluminium is present, chlorite is expected to be an ubiquitous Al-rich phase throughout greenschist, amphibolite, and eclogite facies metamorphism of ultramafic rocks. When a lherzolite or a pyrolite composition is considered, i.e., where Ca and Na are more abundant, a calcic amphibole can be present. At temperatures within the chlorite stability field, amphibole is expected to be relatively Al poor, i.e., tremolitic in greenschist facies as reported in a large number of examples from ophiolites. At temperatures in excess of chlorite stability (≈750–800°C), both Na and Al increase in amphibole as temperature increases, leading to pargasitic compositions (Niida & Green 1998) close to the solidus.

Amphibole breakdown with pressure is located at ≈2.5 GPa at 700°C. Even though such breakdown is commonly regarded as a discrete fluid pulse, it is

fundamental to stress that the migration of amphibole composition from tremolite to progressively more Al-rich composition leads to the fluid-absent reaction

$$amphibole + olivine = chlorite + clinopyroxene + orthopyroxene$$

which is responsible for its disappearance from H_2O-saturated assemblages (Fumagalli 2000). Therefore, at temperatures lower than ≈800°C the release of fluid controlled by amphibole-bearing reactions occurs at relatively low pressures and not exceeding 70 km in depth. Between 800°C and the solidus, the breakdown of amphibole leads to the anhydrous assemblage olivine + orthopyroxene + clinopyroxene + garnet; the exact pressure of amphibole decomposition is a function of Ca and Na contents of the system. Niida & Green (1998) found that amphibole stability extends to 3 GPa at 925°C in an enriched composition corresponding to lherzolite − 40% olivine (5.63 wt% CaO, 0.66 wt% Na_2O, 7.28 wt% Al_2O_3). They also showed that half of the amphibole present at 1 GPa decomposes through a continuous reaction before reaching its terminal pressure stability.

Because of the high dP/dT expected for P-T-t paths in most subduction zones, antigorite and chlorite are the critical volatile-bearing phases in the subducting slab up to pressures of 5 GPa. In principle, talc is restricted to low pressure, but tschermak-substituted talc might occur at somewhat higher pressures. Mass-balance calculations suggest that a maximum of ≈4.5 wt% H_2O is lost when a subducted peridotite moves from the antigorite + chlorite field to the chlorite only field. The importance of antigorite during prograde dehydration of altered peridotites has also been demonstrated by structural and petrological analysis of the relationships between the generation of fluid inclusions and antigorite breakdown in high-pressure peridotites from the Alps (Scambelluri et al. 1997).

Experiments in both MASH and peridotitic compositions reveal that chlorite breaks down above ≈5 GPa to several possible mineral assemblages that are critical for H_2O transfer to large depths. Available experimental data suggest that a 10 Å phase structure may form at $T < 700$°C. Fumagalli & Poli (1999) and Fumagalli et al. (2001) reported for this phase a composition extending toward Al-rich compositions and an unusual swelling behavior that is possibly related to a progressive disruption of chlorite framework to form a mixed-layer mineral whose properties have still to be entirely explored. MgMgAl-pumpellyite (Fockenberg 1998, Artioli et al. 1998) occurs in MASH at $P \geq 5.4$ GPa; however, it is expected to be of only secondary relevance in real peridotitic rocks as a result of the largely extended stability field of garnet s.s. + H_2O. Stalder & Ulmer (2001) recently showed that in MSH even minor amounts of fluorine may enhance the low-pressure, low-temperature stability of clinohumite for a wide range of $MgO:SiO_2$ bulk ratios, and Kawamoto et al. (1996) found Ti-clinohumite at 7.7 GPa, 550°C (coexisting with Ti-chondrodite) and at 9 GPa, 900°C in synthesis performed on a peridotite. Therefore, the prediction of phase relationships above chlorite stability is still vague and certainly strongly affected by presence of minor chemical components such as Ti, F, and Cl. Whatever reaction or mechanism transfers volatiles from antigorite-chlorite bearing assemblages to pressures above 5–6 GPa, once phase

A ($Mg_7Si_2O_8(OH)_6$) appears together with enstatite (Kawamoto et al. 1996) there is no more hindrance for H_2O transport to deep subduction environments (see section 5).

Addition of C to the system enables the appearance of carbonates and/or graphite/diamond, depending on f_{O_2}, and phase equilibria might involve a C-O-H mixed fluid. Stability fields of dolomite and magnesite in systems where CO_2 is the only volatile component are well defined by reactions such as

$$forsterite + CO_2 = enstatite + magnesite$$

and

$$enstatite + dolomite = diopside + magnesite$$

(see Luth 1999 for a review). Excess dolomite is found to decompose to the assemblage magnesite + aragonite at pressures above 5 GPa from 600°C to 900°C (Luth 2001). However, more complex phase relationships including both hydrates and carbonates are still mainly based on theoretical considerations (Kerrick & Connolly 1998).

3.2. Mafic Systems

Extensive petrological work in the early 1980s on the evolution of mafic rocks metamorphosed in blueschist, amphibolite, and eclogite facies (Thompson et al. 1982) has demonstrated that phase relationships in this system are dominated by continuous reactions. Whole-rock composition, therefore, exerts major control on the stability field of mineral assemblages.

At pressures lower than ≈2.5 GPa, a sodic amphibole, chlorite, and albite/clinopyroxene coexist with lawsonite or zoisite along most expected P-T paths for mature subduction zones (Figure 5). Relatively warm paths, possibly related to early stages of subduction, move from chlorite-Na-amphibole bearing assemblages to the amphibole-eclogite field, where Na-Ca amphibole coexist with large amounts of clinopyroxene, and garnet is the aluminous phase in place of chlorite. A quantitative determination of reactions involving chlorite would be important for quantification of the volatile transport; however, such reactions are sluggish and low temperatures hinder a careful experimental investigation.

Experimental studies (Poli 1993, Liu et al. 1996, Pawley & Holloway 1993, Yaxley & Green 1994, Poli & Schmidt 1995, Schmidt & Poli 1998, Molina & Poli 2000) show that amphibole stability in a tholeiitic composition extends to no more than ≈2.5 GPa, both in H_2O-saturated systems and in the presence of a H_2O-CO_2 mixed-fluid. A comparison of the experimental results by Poli (1993), Pawley & Holloway (1993), Liu et al. (1996), and Molina & Poli (2000) indicates that amphibole breakdown moves to slightly higher pressure as X_{Mg} ($X_{Mg} = Mg/(Mg+Fe^{2+})$) increases. Amphibole breakdown at H_2O-saturated conditions may lead to the formation of Mg-rich chloritoid as a result of the reaction

$$amphibole + zoisite = chloritoid + clinopyroxene + quartz + water$$

(Poli 1993). X_{Mg} should have a profound effect on the stability of Mg-chloritoid as well as an indirect effect on epidote. Even though Liu et al. (1996) interpret the occurrence of chloritoid as metastable, results by Poli (1993), Pawley & Holloway (1993), Poli & Schmidt (1995), and Schmidt & Poli (1998) indicate that relatively high X_{Mg} and oxygen fugacities $\leq$NNO should stabilize chloritoid. The most spectacular examples of Mg-chloritoid stability in mafic rocks actually come from Mg-rich differentiates in the Allalin gabbro (Chinner & Dixon 1973). Talc, paragonite, and Mg-staurolite occurrences are also strongly controlled by rock composition, and their amount in P-T-composition space are still poorly defined. Phengite is the ubiquitous potassium phase present at any condition on a pressure-emphasized P-T path.

The potentially huge P-T stability fields of lawsonite and zoisite, ranging from the onset of subduction (Maekawa et al. 1993) down to more than 200 km depth (Poli & Schmidt 1998, Schmidt & Poli 1998, Ono 1998, Okamoto & Maruyama 1999), are therefore responsible for H_2O storage and recycling to depths in excess of amphibole stability in a variety of rock compositions. Their appearance and disappearance are related to complex continuous reactions encountered at variable P-T conditions as a function of $Ca/(Mg + Fe^{2+})$ ratio and H_2O availability. Figure 6 shows how such continuous reactions control variations in hydrate-bearing assemblages even at H_2O-undersaturated conditions, and how the progressive displacement of the composition of an anhydrous solid solution may lead to H_2O-saturation and therefore to fluid release.

The blue surfaces in Figure 6*a*,*b* define the appearance of a fluid toward the H_2O apex and therefore represent H_2O-saturation. A bulk composition below these surfaces will have hydrous phases present but not a fluid. A H_2O-free composition will plot on the base of the CFMASH tetrahedron and correspond to a garnet + clinopyroxene eclogite. The red surfaces in Figure 6 stand for the transformation from the phase field containing both lawsonite and zoisite to the phase field containing only zoisite, which is more H_2O deficient. The progressive displacement of the blue and red surfaces toward a more grossular rich garnet (see also Okamoto & Maruyama 1999) with pressure and temperature causes (for a given bulk composition) either the attainment of fluid saturation (blue pseudo-univariant lines in Figure 6*c*), the appearance of lawsonite via a water-absent reaction (pseudo-univariant lines in red), or simply a variation in the modal abundances of the phases already present. This signifies that at the same P-T condition in some structural and chemical domains of the subducted oceanic crust, lawsonite is consumed to form a free fluid, and in other domains lawsonite is produced from zoisite. When such possible mechanisms are extended to other volatile-bearing assemblages, a very complex pattern of fluid release may result and a simplistic view of fluid flushes at each discontinuous hydrate breakdown is completely unrealistic.

Further complexity is introduced by the presence of carbon as a component and therefore by equilibria involving mixed fluids. Yaxley & Green (1994) and Molina & Poli (2000) showed that hydrates and carbonates coexist in a large P-T range, buffering fluid composition. At fluid saturated conditions, the pressure stability

of amphibole at low temperatures is not significantly affected by the presence of carbon, because this component is strongly fractionated in carbonates and the coexisting fluid is rich in H_2O. Experimental results suggest that calcite is stable at pressures lower than 1.4 GPa, it reacts with amphibole to form dolomite at higher pressures, and magnesite appears at $P \geq 1.8$ GPa.

To conclude this section, a word of caution is mandatory when phase relationships experimentally obtained on a tholeiitic composition are extrapolated to the universe of possible whole-rock compositions present in the oceanic crust. Devolatilization reactions in such variable compositional systems are necessarily diachronous (leading again to a dehydration signal smeared out over a significant depth interval).

3.3. Sediments

The large number of possible mineral assemblages in metapelites and metagreywackes are commonly described in the model system K_2O-FeO-MgO-Al_2O_3-SiO_2-H_2O (KFMASH) $\pm$ CaO or Na_2O (to include the grossular component of garnet, Ca phases such as epidote/zoisite, and feldspar solid solution). As most reactions imply major dehydration, petrogenetic grids are characterized by steep univariant lines in P-T diagrams, and therefore numerous phase assemblages are stable over a large pressure range but in a restricted temperature window (e.g., staurolite + garnet + biotite + muscovite, from a few 100 MPa to almost 1.8 GPa). Despite the systematic work performed on metapelites from "Barrovian" and from high-pressure terrains (Mottana et al. 1990, Liou et al. 1998), enormous differences occur between currently available petrogenetic grids on metasedimentary materials (e.g., White et al. 2001 versus Spear 1993). Such differences mainly arise from the lack of fully reliable thermodynamic data on micas and chlorite, as well as on an ineluctable subjectivity in the interpretation of the evolution of natural phase assemblages and from differences in μ_{H_2O} due to fluid composition. Major differences in phase diagram topologies are related to the stability field of the pair garnet + chlorite (+ muscovite s.s. + quartz + H_2O) and consequently to the P-T location and slope of a number of reactions, including the most controversial: garnet + chlorite = chloritoid + biotite.

Phase relationships to $\approx$3 GPa presented here (Figure 7) are based on experimental work performed at the University of Milan (Valle 1995; Benciolini 1996; Ferri, unpublished data) which is substantially consistent with the topology proposed by Kepezhinskas & Klestov (1977). This topology includes a "prograde" sequence of the pairs garnet + chlorite $\rightarrow$ chloritoid + biotite $\rightarrow$ staurolite + biotite with temperature increase, even at relatively high pressure ($\approx$1.5 GPa) (see Albee 1972). Staurolite breakdown with pressure is located at $\approx$1.7 GPa, and appearance of the characteristic tie-line garnet + talc (Mottana et al. 1990) is expected above $\approx$2.4 GPa in most bulk compositions together with Mg-chloritoid (Schreyer & Chopin 1983), especially in Al-rich compositions. Despite the complex evolution of mineral assemblages buffering the tschermak ($Al_2Mg_{-1}Si_{-1}$) substitution,

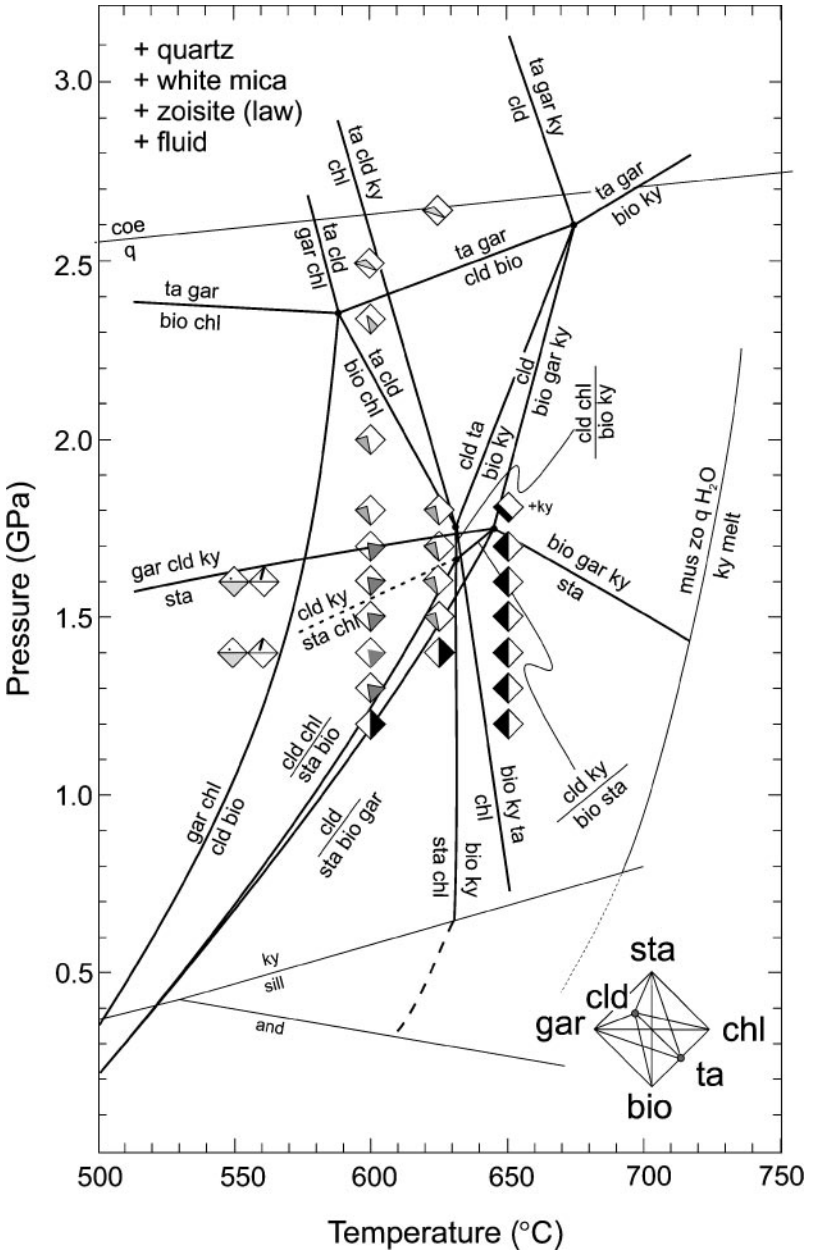

Figure 7 Phase diagram for metasediments at $a_{H_2O} \approx 1$ on the basis of experimental data in the model system CaO-K_2O-FeO-MgO-$Al_2O_3SiO_2$. Solidus from Hoschek 1990.

the Si content in muscovite-phengite solid solutions is expected to increase progressively with pressure (Massone & Schreyer 1987, Schmidt 1996). Because of both the expected shift of phase compositions toward higher X_{Mg} values and the increasing Mg + Fe content in phengite, metasediments show a progressive increase in the modal abundance of garnet with increasing pressure, and conversely, a consumption of biotite. The occurrence of biotite at ultra-high-pressure conditions is therefore restricted to compositions with high X_{Mg} where its stability to $\approx$5 GPa is demonstrated by spectacular intergrowths of biotite with microdiamond in gneisses from the Kokchetav Massif (Sobolev & Shatsky 1990).

The appearance of clinopyroxene in Ca-Na bearing systems is still poorly constrained even though albite breakdown with pressure should represent a lower limit. Transformations from talc + chloritoid ± biotite–bearing assemblages to phengite-eclogites, i.e., to garnet + clinopyroxene + phengite + coesite ± kyanite ± zoisite/lawsonite (Ono 1998, Domanik & Holloway 1996, Schmidt & Vielzeuf 2001), are still poorly understood, even though talc stability is restricted to temperatures lower than 700°C (Hermann 2001). It is worth noting that K-feldspar is always absent at H_2O-saturated conditions; inversely, its occurrence indicates H_2O-undersaturation in the system. The relevance of topaz-OH and MgMgAl-pumpellyite has still to be investigated, even though their presence with phengite to more than 900°C at 7 GPa (Domanik & Holloway 1996, Ono 1998) may imply that metasedimentary materials can transport high amounts of volatiles to much higher P and T than ultramafic or mafic rocks.

4. MELTING OF A SUBDUCTING CRUST

Two modes of melting can be envisioned in subducting crust. As significant amounts of fluid can probably not be retained within a given lithology, fluid-absent melting that relies on the hydrous minerals present (micas, amphibole, zoisite) is the likely melting process. However, the large inverted temperature gradient of >200–300°C within the subducting lithosphere causes underlying lithologies to devolatilize when upper parts of the crust reach melting temperatures. Thus, fluid-saturated melting through flushing with metamorphic fluids (e.g., from serpentine dehydration) can occur.

For the purpose of melting, subducting crust can be chemically divided into a mica-dominated layer (greywackes and pelites) and an amphibole-zoisite dominated layer (mafics). Other sedimentary lithologies (cherts, carbonates) have relatively higher melting temperatures and any carbonate addition through metasomatism increases melting temperatures by decreasing H_2O activity in the fluid or melt. The partially hydrated ultramafic layer might be important as a source of volatiles but does not itself melt. Except in extreme temperature situations (subduction of ridges, Archean subduction), melting temperatures are not reached below approximately 1 GPa, and the following discussion is limited to higher pressures.

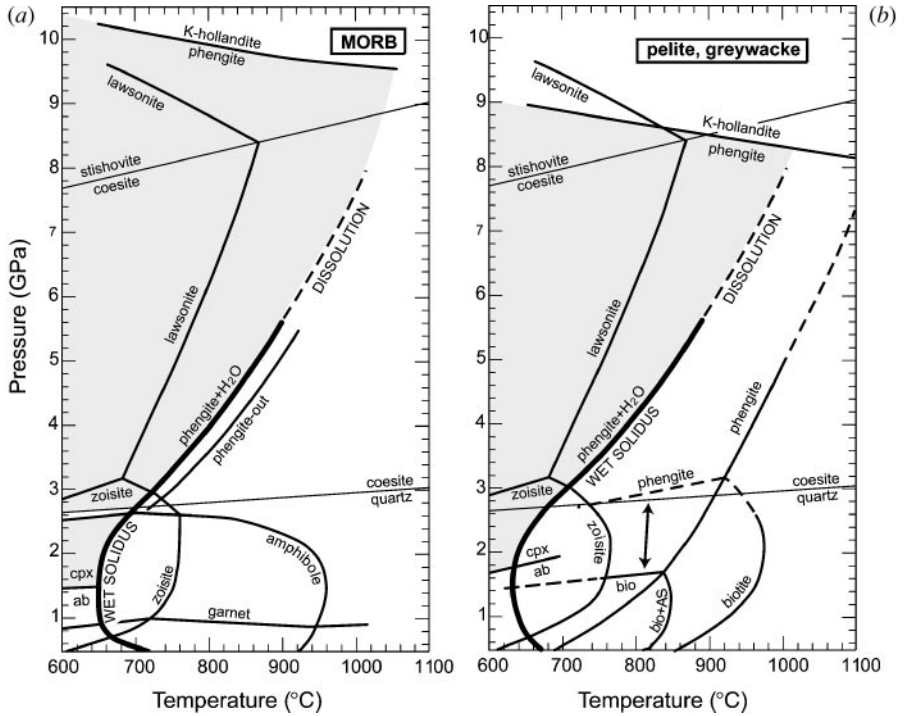

Figure 8 Melting relations in (*a*) MORB and (*b*) terrigenous sediments. (*a*) For pressures of 0.8–3.0 GPa, epidote/zoisite is the first hydrous phase to melt. (*b*) For pressures above 0.4 GPa, muscovite is the first hydrous phase to melt; the appearance of garnet is located at pressures below 0.5 GPa. In both (*a*) and (*b*) phengite is the only hydrous phase at the solidus above 3 GPa. Shaded fields represent the stability of the assemblage phengite + clinopyroxene + coesite ± H_2O. Modified from Vielzeuf & Schmidt (2001); see also Ono (1998), Poli (1993), Schmidt & Vielzeuf (2001), Vielzeuf & Holloway (1988), Winther & Newton (1991), and Wyllie & Wolf 1993.

4.1. Mica-Dominated Sediments

Terrigenous sediments are mostly SiO_2 saturated, but thay are also often Al_2SiO_5 saturated and potassium rich. Micas are the dominant hydrous minerals (typically around 30 vol%), and in a subduction regime the predominant mica is muscovite/phengite. Its stability curve intersects with the wet solidus around 0.4 GPa (Figure 8*b*), and at higher pressures, initial melts will form through the reaction

$$muscovite\ s.s. + albite/jadeite + quartz \pm fluid = biotite + Al_2SiO_5 + melt.$$

The resulting melts are peraluminous; the incongruent melting reaction produces kyanite and biotite (Vielzeuf & Schmidt 2001). To 2.0–2.5 GPa, the assemblage at the solidus is mostly phengite + biotite + plagioclase + garnet + quartz ± kyanite.

At higher pressures the solidus assemblage phengite + jadeitic clinopyroxene + garnet + coesite ± kyanite is identical to the assemblage present in mafic compositions (see below).

Melting of sediments with concomitant dehydration of basalts becomes increasingly popular in geochemistry on the basis of certain isotopes or elements (e.g., Be, Th) that are thought not to be sufficiently mobilized in low-density, low-pressure fluids (bulk fluid/sediment distribution coefficients <0.2–0.5; Johnson & Plank 1999). We argue that this scenario is neither likely nor necessary. (*a*) The postulate on melting of the subducting crust poses a rigid temperature constraint of ≥750–800°C at 2–3 GPa for the interface of the subducting crust with the mantle wedge, and it is statistically unlikely that such conditions are realized in many subduction zones. (*b*) Such high temperatures are substantially incompatible with the currently accepted mechanism for the generation of deep earthquakes (see section 5), which requires temperatures in the order of 600–800°C at transition zone depths. (*c*) The relative proportions of H_2O stored in hydrous minerals (at 60 km depth) of the sedimentary, mafic, and hydrated ultramafic layer are such that the ratio of H_2O between 3 km fully hydrated basalt and 200 m terrigenous sediment is approximately 30. Fluids from the dehydrating basaltic layer migrate upwards through the sediments, and thus a highly increased fluid/rock ratio might leach out these trace elements from the sediments (as it is the case for B, Ryan et al. 1995). (*d*) In addition, with increasing pressure fluids become more solute rich (or even supercritical) and thus are likely to have increased trace element solubilities.

4.2. Metabasalts

Between 1 and 3 GPa, the two most important hydrous minerals in mafic eclogite at solidus temperatures are amphibole (50–30 vol%, decreasing with pressure) and epidote/zoisite (5–15 vol%). Epidote/zoisite is limited to temperatures around 750°C (1.0–2.5 GPa), whereas amphibole decomposes mostly in the temperature range of 850–1000°C (Figure 8*a*). Thus, initial melts produced at fluid-absent conditions are generated through a reaction consuming epidote/zoisite:

$$epidote/zoisite + amphibole + quartz = garnet + melt \pm clinopyroxene$$

(Vielzeuf & Schmidt 2001). Epidote/zoisite melts within a narrow temperature interval; however, the exact stoichiometry of the epidote melting reaction is unknown but is unlikely to produce a large amount of melt. It is possible that only the second major step of melting, i.e., amphibole-dominated fluid-absent melting (Winther & Newton 1991, Wyllie & Wolf 1993), is capable of producing amounts of melt large enough to extract from its host rock. As discussed above, amphibole in mafic compositions is limited to 2.5 GPa and zoisite to 3.0 GPa. Any potassium-free mafic composition is free of hydrous phases at higher pressures and thus classifies as "dry" and "unmeltable" at subduction zone conditions. The only possible remaining hydrous phase at solidus temperatures (at 3–10 GPa) is phengite, the ubiquitous K-phase. The predicate unmeltable

equally applies to hydrate-free, carbonate-bearing mafic eclogites, where melting does not appear before 1200°C at 3.0 GPa (Yaxley 1999, Yaxley & Green 1994).

4.3. An Upper Pressure Limit to Melting?

It appears that for any potassium-bearing eclogite, from greywacke to pelite and from granitic (Huang & Wyllie 1973) to tonalitic (Poli & Schmidt 1995) to mafic, the constituting assemblage on the solidus at ≥3 GPa is phengite + clinopyroxene + garnet + coesite ± kyanite. A classical melting behavior occurs for this assemblage at 4 GPa through a single melting reaction

$$phengite + clinopyroxene + coesite \pm H_2O = melt$$

(Schmidt & Vielzeuf 2001) at temperatures of 850–900 °C, with much higher melt productivities in greywacke or pelite than in MOR basalt. The investigation of the same assemblage at 6.5–7.5 GPa yielded that at near fluid-absent conditions (0.6–1.4 wt% H_2O in excess of what can be stored in phengite) phengite disappears and potassium dissolves entirely in a high density fluid between 1000 and 1150°C. Such fluids contain in excess of 60 wt% dissolved matter and can only be interpreted in terms of a chemical continuum between fluid and melt. The second critical end point (see section 2.2) for the above natural compositions is thus situated around 5 GPa. Quench phases from the above supercritical fluid are K, Al, and Si rich with only minor Na and Fe. Such fluids are thus ideally suited for K-metasomatism in the overlaying mantle wedge [e.g., as observed in Finero, Ivrea Zone (Zanetti et al. 1999)] and will cause phlogopite or K-richterite formation therein (Konzett & Ulmer 1999).

4.4. Melt Compositions

Melt compositions in terms of major and trace elements vary somewhat as a function of the residual assemblage, which is mostly pressure dependent. Melting at low pressures, i.e., below the garnet-in in basalts or pelites (at 1.0–1.2 GPa), occurs only in very special settings; thus, almost any melt derived from a subducted slab has a trace element garnet-signature. At pressures below 2.5–3.0 GPa, melt compositions vary from granodioritic to tonalitic or trondhjemitic (Figure 9) with increasing degree of melting; they are generally sodium rich and just need some olivine absorption during their ascent through the mantle wedge in order to compare well to the adakitic magma suites (see review by Martin 1999). However, clinopyroxene is commonly a residual phase and with increasing pressure becomes more jadeitic, even at elevated temperatures when in equilibrium with melt. Thus, sodium changes its behavior fundamentally and becomes incompatible at high pressure ($D^{Na}_{cpx/melt}$ = 2–6 at 4 GPa) (Schmidt & Vielzeuf 2001). Consequently, slab melts have an increased K/Na ratio with pressure (Figure 9) leading to an enrichment of Na in the eclogitic residue.

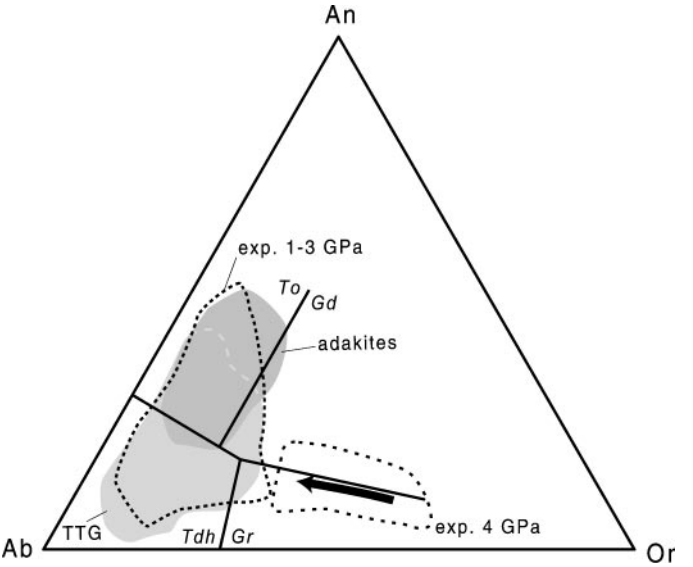

Figure 9 Melt compositions in terms of K-Na-Ca ratios. Fields for modern adakites and Archean TTG [tonalite (To)—trondhjemite (Tdh)—granodiorite (Gd)] from Martin 1999. Gr: granite. Melts at 4 GPa after Schmidt & Vielzeuf 2001, arrow indicates increasing temperature and degree of melting.

5. "DEEP" SUBDUCTION

5.1. Phase Transformations in Deeply Subducting Slabs

The behavior of the subducted slab and of the associated mantle at depths in excess of 400 km reflects the interaction with the mantle transition zone, defined by sharp seismic discontinuities at 400–410 km and 660–670 km depth (hereafter referred to as *410* and *660*). Although these discontinuities are well established, the extents of velocity changes and velocity gradients are still in discussion. Because olivine is the major component in the mantle, most observations attributed to the *410* and *660* are currently reconciled to transformations in the phase diagram of the system Mg_2SiO_4-Fe_2SiO_4 (Akaogi et al. 1998, Fei & Bertka 1999, and references therein). However, complex reactions such as the transformation of Al-bearing majorite ($Mg_3^{VIII}(Mg,Al)^{VI}(Si,Al)^{VI}\,Si_3^{IV}O_{12}$) to Al-perovskite ($((Mg,Al)^{VIII–XII}(Si,Al)^{VI}O_3$) contribute to the transition to the lower mantle (Kubo & Akaogi 2000, Wood 2000, and references therein). The occurrence of an ilmenite structure ($Mg^{VI}Si^{VI}O_3$) at relatively low temperature; the influence of Fe^{2+} (Ohtani et al. 1991, O'Neill & Jeanloz 1994, Faust & Knittle 1996); the complex incorporation of Fe^{3+} in garnets, spinels (Woodland & Angel 2000, and references therein), and perovskite (McCammon 1997); and the equilibria with Ca-perovskite (Irifune

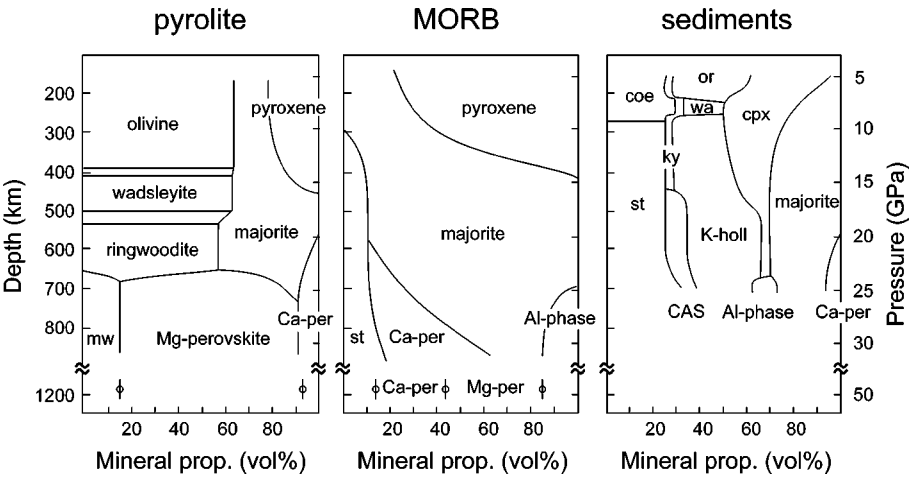

Figure 10 Mineral proportions in pyrolitic mantle and in thermally equilibrated MORB and sediments. After O'Neill & Jeanloz (1990), Irifune & Ringwood (1993, 1994), Kesson et al. (1994).

1994, Gasparik & Drake 1995) introduce further uncertainties on the correlation of seismically detectable discontinuities with phase transformations.

According to the experimental results of Irifune (1994) and Wood (2000) in pyrolitic compositions, majorite breakdown to Mg- and Ca-perovskites should be complete at 24–26 GPa. Mineral abundances calculated at 54 GPa (O'Neill & Jeanloz 1994) (Figure 10) closely match estimations at 26 GPa, suggesting a relative unreactivity of the assemblage perovskites + magnesiowüstite in the upper portion of the lower mantle.

Subducted oceanic lithosphere is characterized by extreme compositional differences. Furthermore, the subducting slab is far from thermal equilibration with the surrounding mantle. Most experimental studies have focused on phase properties and relationships at conditions characteristic of the undisturbed mantle, and therefore our knowledge of what happens in the oceanic lithosphere during deep subduction is still fragmentary. Phase diagrams of the system Mg_2SiO_4-Fe_2SiO_4 indicate that the harzburgite layer of a relatively cold subducted lithosphere undergoes densification at pressures lower than the surrounding mantle, at depths between 350 and 450 km. In comparison, the lower temperatures in the slab cause a deepening of the *660* due to the negative dP/dT-slope of the ringwoodite-perovskite transformation. Depletion of Ca and Al, and therefore presence of a nearly pure $(Mg,Fe)SiO_3$ majorite, are responsible for sharper transitions in harzburgite. On the contrary, higher Fe, Ca, and Al in middle-ocean ridge basalt layers are responsible for the extensive stability of a complex majoritic garnet. Experiments by Irifune & Ringwood (1993) demonstrate that eclogite (pyroxene + garnet) transforms progressively to garnetite (a rock entirely constituted by majoritic

garnet + stishovite) between 10 and 15 GPa (Figure 10). Majorite breakdown begins with exsolution of the Ca-component to give Ca-perovskite [Ca-perovskite garnetite (Okamoto & Maruyama 2001)] through a reaction having a steep positive dP/dT slope. Above 24 GPa, one or more "Al- rich phases" appear in basaltic compositions *s.l.* (Kesson et al. 1994, Faust & Knittle 1996). Composition and crystal structure of this "Al-rich phase" are only approximately determined. A Ca-ferrite structure has been inferred from X-ray powder diffraction, but proposed zero-pressure densities range from 3.87 g/cm^3 (Irifune & Ringwood 1993) to 4.13 g/cm^3 (Kesson et al. 1994). A solid solution between $MgAl_2O_4$ (Funamori et al. 1998), $NaAlSiO_4$, and a tschermak component is possible on the basis of the chemical data reported in Kesson et al. (1994). Majorite-perovskite transformation in MORB compositions has not been systematically investigated yet. Available results by Irifune & Ringwood (1993) and Hirose et al. (1999) are conflicting in the critical region between 25 and 28 GPa, leading to different interpretations of density evolutions and density contrasts with surrounding mantle at depths between 660 and 750 km.

Thermal models of subduction zones predict temperatures within the slab several hundred degrees below those investigated experimentally. Thus, work has still to be done to determine phase boundaries and density changes in the deeply subducted slab. Furthermore, chemical components inherited from the oceanic history of the slab, e.g., H_2O and CO_2, cause the appearance of minor quantities of hydrates or carbonates, which are extremely important from a petrogenetic point of view. Most experiments on hydrates performed in the MgO-SiO_2-H_2O system reveal a number of potential hydrous phases across the transition zone (Ohtani et al. 2000, Frost 1999, Shieh et al. 1998) Among these, phase E ($Mg_{2.1}Si_{1.1}H_{3.6}O_6$), phase B [$Mg_{24}Si_2^{VI}Si_6^{IV}O_{38}(OH)_4$], superhydrous phase B [$Mg_{10}Si^{VI}Si_2^{IV}O_{14}(OH)_4$], and phase D ($MgSi_2^{VI}H_2O_6$) are the most likely hydrous phases (Frost 1999, Ohtani et al. 2000, and references therein). Phase D is the only dense hydrous magnesian silicate with Si entirely in octahedral coordination and is thus stable from 1000°C, 16 GPa to at least 1400°C, 25 GPa; eventually even to 40–50 GPa (Shieh et al. 1998). Occurrence of phase D at transition zone conditions is limited to pressure-temperature paths sufficiently cold to maintain continuous H_2O reservoirs from antigorite to phase A to phase E or superhydrous phase B and finally to phase D. However, as hydrous wadsleyite is capable of containing up to 3.3 wt% H_2O (Kohlstedt et al. 1996), an extensive debate has developed on whether the available hydrogen is completely incorporated in nominally anhydrous minerals or also in a hydrous phase.

Regarding the effect of CO_2 on silicate-bearing assemblages, magnesite appears to be the stable carbonate in a wide spectrum of bulk compositions in the transition zone and lower mantle (Biellmann et al. 1993). The extremely high temperatures of decarbonation for magnesite at conditions of the transition zone and lower mantle suggest that CO_2 is hardly transferred from the subducted slab to the overlaying mantle as a volatile species.

Geochemical signatures of both arc and ocean-island primary magmas require subduction of sediments. Experiments by Irifune & Ringwood (1994) on a

synthetic composition approaching average continental crust provide a first insight on subsolidus phase relationships in K- and Al-rich systems and constraints on melting of sediments at ultra-high-pressure conditions. K-hollandite ($KAlSi_3O_8$) is the potassic phase above 9 GPa and coexists with stishovite, majoritic garnet, pyroxene, and, above 20 GPa, with Ca-perovskite (Figure 10). At the highest pressures investigated, the Al-rich phase with a Ca-ferrite structure was also present. Given that Irifune's starting material contained 2 wt% H_2O, it is worth noting that the temperature of the solidus (evaluated at liquid proportions lower than 5 vol.%) may be overstepped only at pressures below ≈10 GPa (when compared to an average mantle adiabat).

5.2. "Deflection" Versus "Penetration" at the 660-km Discontinuity

In order to understand whether the subducted slab penetrates the 660-km discontinuity or accumulates at the bottom of the transition zone, we need a combined geophysical, geochemical, and petrological approach, including the evaluation of buoyancy forces at the 660-km discontinuity, modeling of thermomechanical properties of the slab and of the surrounding mantle across the *660*, comparison between predicted mantle mechanics and seismic tomography modeling, analysis of chemical and isotopic signatures of ocean island basalts (OIB) and the genesis of deep plumes, and a number of time-dependent constraints (e.g., isotopic evolution; see Christensen & Hofmann 1994).

Slab behavior is strongly affected by the density distribution and therefore by the buoyancy force acting on the slab. The simplest way to obtain an excess density is to introduce a temperature contrast. A more complex density contrast is caused by differences in phase assemblages or phase abundances. These, in turn, are the result of differences in temperature and pressure and/or chemical composition. Temperature dependence of a phase transformation can be formulated as (Clapeyron law): $dP/dT = \Delta H/(T\Delta V)$, where ΔH and ΔV are the enthalpy and volume differences of the phase transformation, and T is the equilibrium temperature. Thus, endothermic ($\Delta H < 0$) transformations with depth have a negative dP/dT, i.e., they generate a positive buoyancy force that impedes convection (Figure 11). On the contrary, a positive dP/dT will assist convection. Phase equilibria discussed in the previous section have $dP/dT \neq 0$, and therefore an elevation, or conversely a depression, of the transition between layers of different phase assemblages (i.e., densities) is generated (Figure 11).

Because the transformation from ringwoodite to perovskite + (Mg,Fe)O has a negative dP/dT of ≈ -3 MPa/K, and because majorite in the crustal layer extends to more than 800 km depth at thermally equilibrated conditions, it has been argued that subducted lithosphere cannot penetrate into the lower mantle, but deflects and accumulates at the *660*. Nevertheless, numerical simulations of mantle flow (Tackley et al. 1993) show that if a total of 9% $\Delta\rho/\rho$ at 660 km depth is assumed, then the critical dP/dT value that defines the transition from whole-mantle

convection (lower dP/dT) to a two-layer regime (higher negative dP/dT) is on the order of -3 to -4 MPa/K. As this value is of the same magnitude as the transformation of ringwoodite, slab penetration might be mostly controlled by phase equilibria involving relatively less abundant phases. If subduction into the lower mantle occurs, once majorite is completely transformed to perovskite and possibly Ca-ferrite, the mafic crust is again denser than a reference PREM [preliminary reference Earth model (Dziewonski & Anderson 1981)] mantle (by $\approx$0.06 g cm^{-3}; Kesson et al. 1994) and should not find any further barrier to deep penetration into the lower mantle (Figure 12).

Buoyancy is the major force controlling the subducted slab across the *660*; however, other relevant factors should not be neglected. Estimates of the rheological properties of garnetite (MORB) compared to wadsleyite/ringwoodite- and perovskite-rich assemblages (pyrolite and harzburgite) (Karato et al. 1995, Ji & Zhao 1994) reveal that creep strength of garnetite is at least one order of magnitude higher than that of the surrounding pyrolite, even at thermally equilibrated conditions. Temperature differences between the cold garnetite layer of the subducted crust and the hot mantle pyrolite largely increase these strength differences. If the density contrasts are relatively low, rheological properties can be decisive. Thicker, older, and faster oceanic plates (cold slabs) are stiff and might penetrate the *660* even if they remain buoyant over a few tenths of a kilometer (Ji & Zhao 1994). Other parameters, such as hydrogen-induced weakening (Kohlstedt et al. 1996 and references therein), are still to be explored.

Most models of slab behavior across the transition zone assume that equilibrium assemblages develop within the subducted slab. If temperatures as low as 600°C are possible in the coldest portion of the slab in the transition zone, it is

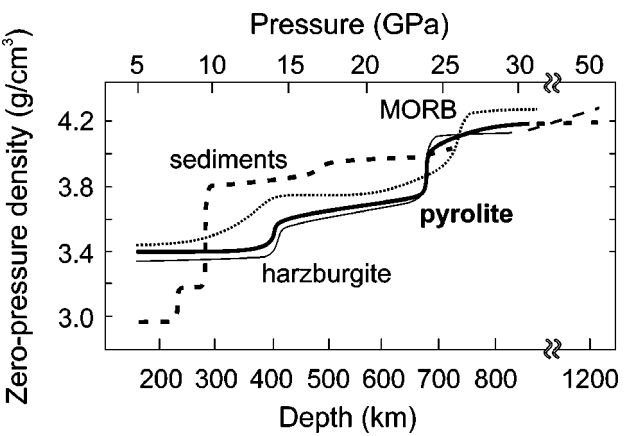

Figure 12 Zero-pressure density in pyrolite and in the main compositional layers of a thermally equilibrated subducted lithosphere. The dashed line is after Irifune & Ringwood 1993, Irifune et al. 1994, and Hirose et al. 1999.

questionable if reaction kinetics allows for complete equilibration of the slab interior. Laboratory experiments (Rubie & Ross 1994, Hogrefe et al. 1994) suggest that the transformations between olivine, wadsleyite, and ringwoodite, and between enstatite and majorite, are inhibited at such temperatures, and a zone of metastable phases occurs. Metastable transformation of olivine (and/or enstatite) to higher-density phases also has important consequences on deep seismicity (400–700 km depth) via the so-called transformational faulting, or anticrack failure (Burnley et al. 1991, Kirby et al. 1991), which is a failure process that takes place when a nonhydrostatic stress acts on a metastable aggregate within the stability field of a denser mineral assemblage.

All parameters and properties discussed above focus on dynamic properties across the transition zone. However, kinematics of plate motion may also affect slab behavior at the *660* (Griffiths et al. 1995 and references therein). Once the slab reaches a depth where the majorite-to-perovskite transformation in the mafic layer has completed, it should sink down to the bottom of the lower mantle, i.e., the core-mantle boundary (CMB). The 200 km thick D″ layer above the CMB is characterized by vertical and lateral variations in compressional and shear wave velocities. A common feature of the D″ in seismic studies is the discontinuous increase in velocity at the top of the layer, which can be attributed to either a thermal boundary layer, a chemical change, or a mineralogical phase transition such as the decomposition of perovskite to magnesiowüstite + stishovite. Even though there is still debate on the complex topography of the D″, the accumulation of subducted lithosphere may cause the concomitant action of all of these mechanisms and explain the dramatic change in physical properties close to the CMB (Wysession et al. 1998).

LITERATURE CITED

Akaogi M, Kojitani H, Matsuzaka K, Suzuki T, Ito E. 1998. Postspinel transformations in the system Mg_2SiO_4-Fe_2SiO_4: element partitioning, calorimetry, and thermodynamic calculation. In *Properties of Earth and Planetary Materials at High Pressure and Temperature*, ed. MH Manghnani, T Yagi, *Geophys. Monogr. Ser.* 101:373–91. Washington, DC: Am. Geophys. Union. 562 pp.

Albee AL. 1972. Metamorphism of pelitic schists; reaction relations of chloritoid and staurolite. *Geol. Soc. Am. Bull.* 83:3249–68

Alt JC. 1995. Subseafloor processes in mid-ocean ridge hydrothermal systems. In *Seafloor Hydrothermal Systems: Physical, Chemical, Biological, and Geological Interactions*, ed. SE Humphris, RE Zierenberg, LS Mullineaux, RE Thomson, *Geophys. Monogr. Ser.* 91:85–114. Washington, DC: Am. Geophys. Union

Artioli G, Fumagalli P, Poli S. 1998. The crystal structure of $Mg_8(Mg_2Al_2)Al_8Si_{12}(O,OH)_{56}$ pumpellyite and its relevance in ultramafic systems at high pressure. *Am. Mineral.* 84: 1906–14

Benciolini N. 1996. *Relazioni di fase in metapeliti ad alta pressione: studio sperimentale.* PhD thesis. Univ. Milano, Milano. 148 pp.

Biellmann C, Gillet P, Guyot F, Peyronneau J, Reynard B. 1993. Experimental evidence

for carbonate stability in the Earth's lower mantle. *Earth Planet. Sci. Lett.* 118:31–41

Boettcher AL, Wyllie PJ. 1969. The system CaO-SiO_2-CO_2-H_2O; III, second critical endpoint on the melting curve. *Geochim. Cosmochim. Acta* 33:611– 32

Bonatti E, Emiliani C, Ferrara G, Honnorez J, Rydell H. 1974. Ultramafic-carbonate breccias from the equatorial Mid Atlantic ridge. *Mar. Geol.* 16:83–102

Boudier F, Nicolas A. 1995. Nature of the Moho transition zone in the Oman ophiolite. *J. Petrol.* 36:777–96

Brenan JM, Shaw HF, Ryerson FJ, Phinney DL. 1995. Mineral-aqueous fluid partitioning of trace elements at 900°C and 2.0 GPa: constraints on the trace element chemistry of mantle and deep crustal fluids. *Geochim. Cosmochim. Acta* 59:3331–50

Bureau H, Keppler H. 1999. Complete miscibility between silicate melts and hydrous fluids in the upper mantle; experimental evidence and geochemical implications. *Earth Planet. Sci. Lett.* 165:187–96

Burnley PC, Green HW II, Prior DJ. 1991. Faulting associated with the olivine to spinel transformation in Mg_2GeO_4 and its implications for deep-focus earthquakes. *J. Geophys. Res.* 96:425–43

Cannat M. 1993. Emplacement of mantle rocks in the seafloor at mid-ocean ridges. *J. Geophys. Res.* 98:4163–72

Chinner GA, Dixon JE. 1973. Some high-pressure paragenesis of the Allalin Gabbro, Valais, Switzerland. *J. Petrol.* 14:185–202

Christensen UR, Hofmann AW. 1994. Segregation of subducted oceanic crust in the convecting mantle. *J. Geophys. Res.* 99:19867–84

Connolly JAD, Cesare B. 1996. C-O-H-S fluid composition and oxygen fugacity in graphitic metapelites. *J. Metamorph. Geol.* 11:379–88

Constantin M. 1999. Gabbroic intrusions and magmatic metasomatism in harzburgites from the Garrett transform fault: implications for the nature of the mantle-crust transition at fast spreading ridges. *Contrib. Mineral. Petrol.* 136:111–30

Davies JH, Stevenson DJ. 1992. Physical model of source region of subduction zone volcanics. *J. Geophys. Res.* 97:2037–70

Domanik KJ, Holloway JR. 1996. The stability and composition of phengitic muscovite and associated phases from 5.5 to 11 GPa; implications for deeply subducted sediments. *Geochim. Cosmochim. Acta* 60:4133–50

Dziewonski AM, Anderson DL. 1981. Preliminary reference Earth model. *Phys. Earth. Planet. Int.* 25:297–356

Faust J, Knittle E. 1996. The stability and equation of state of majoritic garnet synthesized from natural basalt at mantle conditions. *Geophys. Res. Lett.* 23:3377–80

Fei Y, Bertka CM. 1999. Phase transitions in the Earth's mantle and mantle mineralogy. See Fei et al. 1999, pp. 189–207

Fei Y, Bertka CM, Mysen BO, eds. 1999. *Mantle Petrology: Field Observations and High Pressure Experimentation: A Tribute to Francis R.* (*Joe*) *Boyd, Spec. Publ. 6*. Houston: Geochem. Soc. 322 pp.

Fockenberg T. 1998. An experimental study of the pressure-temperature stability of MgMgAl-pumpellyite in the system MgO-Al_2O_3-SiO_2-H_2O. *Am. Mineral.* 83:220–27

Frost DJ. 1999. The stability of dense hydrous magnesium silicates in Earth's transition zone and lower mantle. See Fei et al. 1999, pp. 283–96

Fumagalli P. 2000. *Processi di trasporto e rilascio di H_2O nelle zone di subduzione: uno studio sperimentale su sistemi ultrafemici ad alta pressione*. PhD thesis. Univ. Milano, Milano. 178 pp.

Fumagalli P, Poli S. 1999. Phase relationships in hydrous peridotites at high pressure: preliminary results of multianvil experiments. *Period. Mineral.* 68:275–86

Fumagalli P, Stixrude L, Poli S, Snyder D. 2001. The 10Å phase: a high- pressure expandable sheet silicate stable during subduction of hydrated lithosphere. *Earth Planet. Sci. Lett.* 186:125–41

Funamori N, Jeanloz R, Nguyen JH, Kavner A, Caldwell WA, et al. 1998. High- pressure transformations in $MgAl_2O_4$. *J. Geophys. Res.* 103:20183–218

Gasparik T, Drake MJ. 1995. Partitioning of elements among two silicate perovskites, superphase B, and volatile-bearing melt at 23 GPa and 1500–1600°C. *Earth. Planet. Sci. Lett.* 134:307–18

Gente P, Pockalny RA, Durand C, Deplus C, Maia M, et al. 1995. Characteristics and evolution of the segmentation of the mid-atlantic ridge between 20°N and 24°N during the last 10 million years. *Earth Planet. Sci. Lett.* 129:55–71

Griffiths RW, Hackney RI, van der Hilst RD. 1995. A laboratory investigation of effects of trench migration on the descent of subducted slabs. *Earth Planet. Sci. Lett.* 133:1–17

Hekinian R, Bideau D, Francheteau J, Cheminee JL, Armijo R, et al. 1993. Petrology of the East Pacific Rise crust and upper mantle exposed in Hess Deep (eastern equatorial Pacific). *J. Geophys. Res.* 98:8069–94

Hermann J. 2001. Experimental constraints on phase relations in subducted continental crust. *Contrib. Mineral. Petrol.* In press

Hirose K, Fei YW, Ma YZ, Mao HK. 1999. The fate of subducted basaltic crust in the Earth's lower mantle. *Nature* 397:53–56

Hirose K, Fei YW, Ono S, Yagi T, Funakoshi K. 2001. In situ measurements of the phase transition boundary in $Mg_3Al_2Si_3O_{12}$: implications for the nature of the seismic discontinuities in the Earth's mantle. *Earth Planet. Sci. Lett.* 184:567–73

Hogrefe A, Rubie DC, Sharp TG, Seifert F. 1994. Metastability of enstatite in deep subducting lithosphere. *Nature* 372:351–53

Hoschek G. 1990. Melting and subsolidus reactions in the system K_2O-CaO-MgO-Al_2O_3-SiO_2-H_2O; experiments and petrologic application. *Contrib. Mineral. Petrol.* 105:393–402

Huang WL, Wyllie PJ. 1973. Melting relations of muscovite-granite to 35 kbar as a model for fusion of metamorphosed subducted oceanic sediments. *Contrib. Mineral. Petrol.* 42:1–14

Irifune T. 1994. Absence of an aluminous phase in the upper part of the Earth's lower mantle. *Nature* 370:131–33

Irifune T, Ringwood AE. 1993. Phase transformations in subducted oceanic crust and buoyancy relationships at depths of 600–800 km in the mantle. *Earth Planet. Sci. Lett.* 117:101–10

Irifune T, Ringwood AE, Hibberson WO. 1994. Subduction of continental crust and terrigenous and pelagic sediments: an experimental study. *Earth Planet. Sci. Lett.* 126: 351–68

Ito E, Sato H. 1992. Effect of phase transformations on the dynamics of the descending slab. In *High-Pressure Research: Application to Earth and Planetary Sciences*, ed. Y Syono, MH Manghnani, *Geophys. Monogr. Ser.* 67:257–62. Washington, DC: Am. Geophys. Union. 530 pp.

Ji S, Zhao P. 1994. Layered rheological structure of subducting oceanic lithosphere. *Earth Planet. Sci. Lett.* 124:75–94

Johnson MC, Plank T. 1999. Dehydration and melting experiments constrain the fate of subducted sediments. *Geochem. Geophys. Geosyst.* 1.

Karato S, Wang Z, Liu B, Fujino K. 1995. Plastic deformation of garnets: systematics and implications for the rheology of the mantle transition zone. *Earth Planet. Sci. Lett.* 130:13–30

Kawamoto T, Hervig RL, Holloway JR. 1996. Experimental evidence for a hydrous transition zone in the early Earth's mantle. *Earth Planet. Sci. Lett.* 143:587–92

Kennedy GC, Wasserburg GJ, Heard HC, Newton RC. 1962. The upper three-phase region in the system SiO_2-H_2O. *Am. J. Sci.* 260:501–21

Kepezhinskas KB, Klestov VV. 1977. The petrogenetic grid and subfacies for middle-temperature metapelites. *J. Petrol.* 18:114–43

Keppler H. 1996. Constraints from partitioning experiments on the composition of subduction-zone fluids. *Nature* 380:237–40

Kerrick DM, Connolly JAD. 1998. Subduction of ophicarbonates and recycling of CO_2 and H_2O. *Geology* 26:375–78

Kesson SE, Fitz Gerald JD, Shelley JMG. 1994. Mineral chemistry and density of

subducted basaltic crust at lower-mantle pressures. *Nature* 372:767–69

Kincaid C, Sacks IS. 1997. Thermal and dynamical evolution of the upper mantle in subduction zones. *J. Geophys. Res.* 102:12295–315

Kirby SH, Durham WB, Stern LA. 1991. Mantle phase changes and deep-earthquake faulting in subducting oceanic lithosphere. *Science* 252:216–25

Kohlstedt DL, Keppler H, Rubie DC. 1996. Solubility of water in the α, β, and γ phases of $(Mg,Fe)_2SiO_4$. *Contrib. Mineral. Petrol.* 123:345–57

Konzett J, Ulmer P. 1999. The stability of hydrous potassic phases in lherzolite mantle; an experimental study to 9.5 GPa in simplified and natural bulk compositions. *J. Petrol.* 40:629–52

Kubo A, Akaogi M. 2000. Post-garnet transitions in the system $Mg_4Si_4O_{12}$-$Mg_3Al_2Si_3O_{12}$ up to 28 GPa: phase relations of garnet, ilmenite and perovskite. *Phys. Chem. Mineral.* 121:85–102

Liou JG, Zhang RY, Ernst WG, Rumble D III, Maruyama S. 1998. High pressure minerals from deeply subducted metamorphic rocks. In *Ultrahigh-Pressure Mineralogy: Physics and Chemistry of the Earth's Deep Interior*, ed. RJ Hemley. *Rev. Mineral.* 37:33–96. Washington, DC: Mineral. Soc. Am. 671 pp.

Liu J, Bohlen SR, Ernst WG. 1996. Stability of hydrous phases in subducting oceanic crust. *Earth Planet. Sci. Lett.* 143:161–71

Luth RW. 1999. Carbon and carbonates in the mantle. See Fei et al. 1999, pp. 297–316

Luth RW. 2001. Experimental determination of the reaction paragonite + magnesite = dolomite at 5 to 9 GPa. *Contrib. Mineral. Petrol.* 14:222–32

Maekawa H, Shozui M, Ishii T, Fryer P, Pearce JA. 1993. Blueschist metamorphism in an active subduction zone. *Nature* 364:520–23

Magenheim AJ, Spivack AJ, Michael PJ, Gieskes JM. 1995. Chlorine stable-isotope composition of the oceanic crust—implications for Earth's distribution of chlorine. *Earth Planet. Sci. Lett.* 131:427–32

Martin H. 1999. Adakitic magmas: modern analogues of Archean granitoids. *Lithos* 46:411–29

Massone HJ, Schreyer W. 1987. Phengite geobarometry based on the limiting assemblage with K-feldspar, phlogopite, and quartz. *Contrib. Mineral. Petrol.* 96:212–24

McCammon C. 1997. Perovskite as a possible sink for ferric iron in the lower mantle. *Nature* 387:694–96

Molina JF, Poli S. 2000. Carbonate stability and fluid composition in subducted oceanic crust: an experimental study on H_2O-CO_2-bearing basalts. *Earth Planet. Sci. Lett.* 176:295–310

Mottana A, Carswell DA, Chopin C, Oberhansli R. 1990. Eclogite facies mineral paragenesis. In *Eclogite Facies Rocks*, ed. DA Carswell, pp. 14–52. New York: Blackie

Nakamura Y, Kushiro I. 1974. Composition of the gas phase in Mg_2SiO_4-SiO_2-H_2O at 15 kbar. *Carnegie Inst. Wash. Yearb.* 73:255–58

Niida K, Green DH. 1998. Stability and chemical composition of pargasitic amphibole in MORB pyrolite under upper mantle conditions. *Contrib. Mineral. Petrol.* 135:18–40

Ohtani E, Kagawa N, Fujino K. 1991. Stability of majorite $(Mg,Fe)SiO_3$ at high pressures and 1800°C. *Earth Planet. Sci. Lett.* 102:158–66

Ohtani E, Mizobata H, Yurimoto H. 2000. Stability of dense hydrous magnesium silicate phases in the systems Mg_2SiO_4-H_2O and $MgSiO_3$-H_2O at pressures up to 27 GPa. *Phys. Chem. Mineral.* 27:533–44

Okamoto K, Maruyama S. 1999. The high-pressure synthesis of lawsonite in the MORB + H_2O system. *Am. Mineral.* 84:362–73

Okamoto K, Maruyama S. 2001. The eclogite-garnetite transformation in the MORB+H_2O system. *Earth Planet. Sci. Lett.* Submitted

O'Neill B, Jeanloz R. 1994. $MgSiO_3$-$FeSiO_3$-Al_2O_3 in the Earth's lower mantle: perovskite and garnet at 1200 km depth. *J. Geophys. Res.* 99:19901–15

Ono S. 1998. Stability limits of hydrous minerals in sediment and mid-ocean ridge basalt compositions: implications for water

transport in subduction zones. *J. Geophys. Res.* 103:18253–67

Pawley AR, Holloway JR. 1993. Water sources for subduction zone volcanism—new experimental constraints. *Science* 260:664–67

Plank T, Langmuir CH. 1998. The chemical composition of subducting sediment and its consequences for the crust and mantle. *Chem. Geol.* 145:325–94

Poli S. 1993. The amphibolite-eclogite transformation—an experimental-study on basalt. *Am. J. Sci.* 293:1061–107

Poli S, Schmidt MW. 1995. H_2O transport and release in subduction zones—experimental constraints on basaltic and andesitic systems. *J. Geophys. Res.* 100:22299–314

Poli S, Schmidt MW. 1997. The high-pressure stability of hydrous phases in orogenic belts: an experimental approach on eclogite-forming processes. *Tectonophysics* 273:169–84

Poli S, Schmidt MW. 1998. The high-pressure stability of zoisite and phase relationships of zoisite-bearing assemblages. *Contrib. Mineral. Petrol.* 130:162–75

Rea DK, Ruff LJ. 1996. Composition and mass flux of sediment entering the world's subduction zones: implications for global sediment budgets, great earthquakes, and volcanism. *Earth Planet. Sci. Lett.* 140:1–12

Rubie DC, Ross CR II. 1994. Kinetics of the olivine-spinel transformation in subducting lithosphere: experimental constraints and implications for deep slab processes. *Phys. Earth Planet. Int.* 86:223–41

Ryan JG, Morris J, Tera F, Leeman WP, Tsvetkov A. 1995. Cross-arc geochemical variations in the Kurile arc as a function of depth. *Science* 270:625–27

Scambelluri M, Philippot P. 2001. Deep fluids in subduction zones. *Lithos* 55:213–27

Scambelluri M, Piccardo GB, Philippot P, Robbiano A, Negretti L. 1997. High salinity fluid inclusions formed from recycled seawater in deeply subducted alpine serpentinite. *Earth Planet. Sci. Lett.* 148:485–99

Schmidt MW. 1996. Experimental constraints on recycling of potassium from subducted oceanic crust. *Science* 272:1927–30

Schmidt MW, Poli S. 1998. Experimentally based water budgets for dehydrating slabs and consequences for arc magma generation. *Earth Planet. Sci. Lett.* 163:361–79

Schmidt MW, Vielzeuf D. 2001. How to generate a mobile component in subducting crust: melting vs. dissolution processes. In *11th Annu. V.M. Golschmidt Conf.*, Abstr. 3366. LPI Contrib. No. 1088, Lunar Planet. Inst., Houston (CD-ROM)

Schneider ME, Eggler DH. 1986. Fluids in equilibrium with peridotite minerals; implications for mantle metasomatism. *Geochim. Cosmochim. Acta* 50:711–24

Schreyer W, Chopin C. 1983. Magnesiocarpholite and magnesiochloritoid; two index minerals of pelitic blueschists and their preliminary phase relations in the model system MgO-Al_2O_3-SiO_2-H_2O. *Am. J. Sci.* 283A:72–96

Sciuto PF, Ottonello G. 1995. Water-rock interaction on Zabargad Island, Red Sea—a case study: I. Application of the concept of local equilibrium. *Geochim. Cosmochim. Acta* 59:2187–206

Shieh SR, Mao H, Hemley RJ, Ming LC. 1998. Decomposition of phase D in the lower mantle and the fate of dense hydrous silicates in subducting slabs. *Earth Planet. Sci. Lett.* 159:13–23

Shmulovic K, Graham C, Yardly B. 2001. Quartz, albite and diopside solubilities in H_2O-NaCl and H_2O-CO_2 fluids at 0.5–0.9 GPa. *Contrib. Mineral. Petrol.* 141:95–108

Snow JE, Dick HJB. 1995. Pervasive magnesium loss by marine weathering of peridotite. *Geochim. Cosmochim. Acta* 59:4219–35

Sobolev NV, Shatsky VS. 1990. Diamond inclusions in garnets from metamorphic rocks—a new environment for diamond formation. *Nature* 343:742–46

Spear FS. 1993. *Metamorphic Phase Equilibria and Pressure-Temperature-Time Paths*. Washington, DC: Mineral. Soc. Am. 799 pp.

Stalder R, Ulmer P. 2001. Phase relations of a serpentine composition between 5 and 14 GPa: significance of clinohumite and phase E as water carriers into the transition

zone. *Contrib. Mineral. Petrol.* 140:670–79

Stalder R, Ulmer P, Thompson AB, Gunther D. 2000. High pressure fluids in the system $MgO\text{-}SiO_2\text{-}H_2O$ under upper mantle conditions. *Contrib. Mineral. Petrol.* 140:607–18

Staudigel J, Plank T, White B, Schmincke HU. 1996. Geochemical fluxes during seafloor alteration of the basaltic upper oceanic crust: DSPDP sites 417 and 418. In *Subduction, Top to Bottom*, ed. GE Bebout, DW Scholl, SH Kirby, JP Platt, *Geophys. Monogr. Ser.* 96:19–38. Washington, DC: Am. Geophys. Union. 384 pp.

Tackley PJ, Stevenson DJ, Glatzmaier GA, Schubert G. 1993. Effect of an endothermic phase transition at 670 km depth in a spherical model of convection in the Earth's mantle. *Nature* 361:699–704

Taylor SR, McLennan SM. 1985. *The Continental Crust: Its Composition and Evolution*. Oxford: Blackwell Sci. Publ.

Thompson JB, Laird J, Thompson AB. 1982. Reactions in amphibolite, greenschist and blueschist. *J. Petrol.* 23:1–27

Ulmer P, Trommsdorff V. 1999. Phase relations of hydrous mantle subducting to 300 km. See Fei et al. 1999, pp. 259–81

Valle M. 1995. *Il sistema metapelitico ad alta pressione: studio sperimentale*. PhD thesis. Univ. Milano, Milano. 130 pp.

Vielzeuf D, Holloway JR. 1988. Experimental determination of the fluid-absent melting relations in the pelitic system. *Contrib. Mineral. Petrol.* 98:257–76

Vielzeuf D, Schmidt MW. 2001. Melting relations in hydrous systems revisited: application to metapelites, metagreywackes and metabasalts. *Contrib. Mineral. Petrol.* 141: 251–67

von Huene R, Scholl DW. 1991. Observations at convergent margins concerning sediment subduction, subduction erosion, and the growth of continental crust. *Rev. Geophys.* 29:279–316

White RW, Powell R, Holland TJB, Worley BA. 2001. The effect of TiO_2 and Fe_2O_3 on metapelitic assemblages at greenschist and amphibolite facies conditions: mineral equilibria calculations in the system $K_2O\text{-}FeO\text{-}MgO\text{-}Al_2O_3\text{-}SiO_2\text{-}H_2O\text{-}TiO_2\text{-}Fe_2O_3$. *J. Metamorph. Geol.* 18:497–511

Winther KT, Newton RC. 1991. Experimental melting of hydrous low-K tholeiite: evidence on the origin of Archean cratons. *Bull. Geol. Soc. Denmark* 39:497–515

Wood BJ. 2000. Phase transformations and partitioning relations in peridotite under lower mantle conditions. *Earth Planet. Sci. Lett.* 174:341–54

Woodland AB, Angel RJ. 2000. Phase relations in the system fayalite-magnetite at high pressures and temperatures. *Contrib. Mineral. Petrol.* 139:734–47

Wunder B. 1998. Equilibrium experiments in the system $MgO\text{-}SiO_2\text{-}H_2O$ (MSH): stability fields of clinohumite-OH [$Mg_9Si_4O_{16}(OH)_2$], chondrodite-OH [$Mg_5Si_2O_8(OH)_2$] and phase A ($Mg_7Si_2O_8(OH)_6$). *Contrib. Mineral. Petrol.* 132:111–20

Wyllie PJ, Wolf MB. 1993. Amphibolite dehydration melting: sorting out the solidus. In *Magmatic Processes and Plate Tectonics*, ed. HM Prichard, T Alabaster, NBW Harris, CR Neary, *Geol. Soc. Spec. Publ.* 76:405–16. London: Geol. Soc. London

Wysession ME, Lay T, Revenaugh J, Williams Q, Garnero EJ, et al. 1998. The D″ discontinuity and its implications. In *The Core-Mantle Boundary Region*, ed. M Gurnis, ME Wysession, E Knittle, BA Buffett, *Geodyn. Ser.* 28:273– 97. Washington, DC: Am. Geophys. Union. 334 pp.

Yaxley GM. 1999. Phase relations of carbonated eclogite under upper mantle PT conditions—implications for carbonatite petrogenesis. In *Proc. 7th Int. Kimberlite Conf. Cape Town*, pp. 933–39

Yaxley GM, Green DH. 1994. Experimental demonstration of refractory carbonate-bearing eclogite and siliceous melt in the subduction regime. *Earth Planet. Sci. Lett.* 128:313–25

Zanetti A, Mazzucchelli M, Rivalenti G, Vannucci R. 1999. The Finero phlogopite-peridotite massif: an example of subduction-related metasomatism. *Contrib. Mineral. Petrol.* 134:107–22

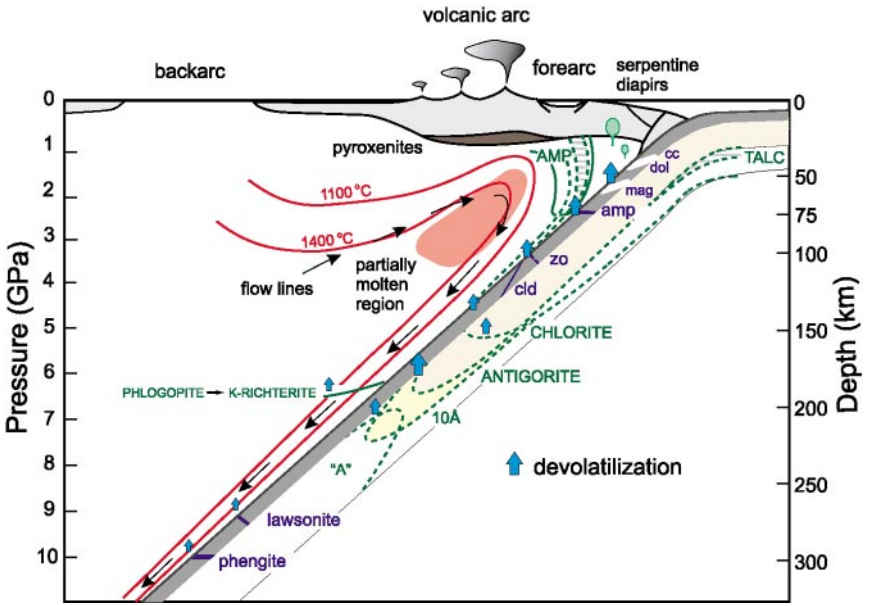

Figure 1 Schematic arrangements of major processes governing subduction zone dynamics. Mineral labels represent the potential stability fields of volatile-bearing phases. The location of partially molten region is constrained by seismic tomography (Zhao 2000). Modified from Schmidt & Poli 1998.

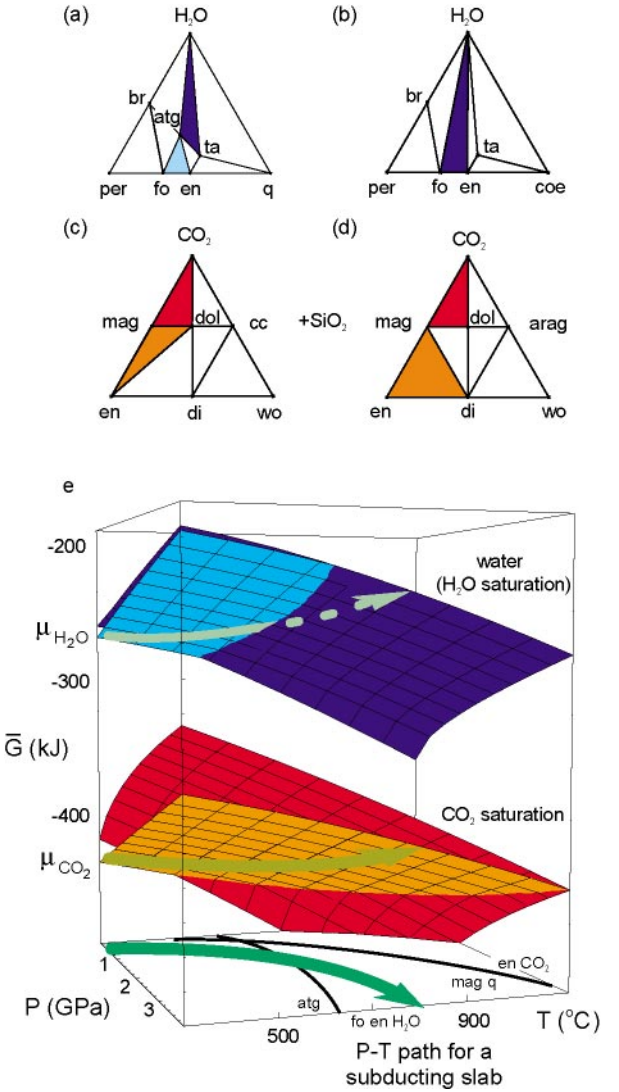

Figure 4 Dehydration and decarbonation along a hypothetical P-T path for subducting slabs. (*a*,*b*) MgO-SiO_2-H_2O chemographies. Assemblages below the tie-lines brucite-antigorite-talc-quartz in (*a*) are H_2O-undersaturated. (*c*,*d*) MgO-CaO-CO_2 projected from SiO_2. Assemblages below the tie-lines magnesite-dolomite-aragonite are CO_2-undersaturated. (*e*) Saturation surfaces for water and carbon dioxide compared to chemical potentials of H_2O and CO_2 buffered by antigorite-enstatite-forsterite (*light blue*) and by magnesite-quartz-enstatite (*orange*), respectively. Volatile saturation and therefore fluid release occurs if the P-T path drives μ_{H2O} or μ_{CO2} toward the thermodynamic surfaces of H_2O- or CO_2-fluid, respectively. Note that $G = \mu_i$. Color of surfaces in (*e*) are keyed to colors in (*a*) through (*d*).

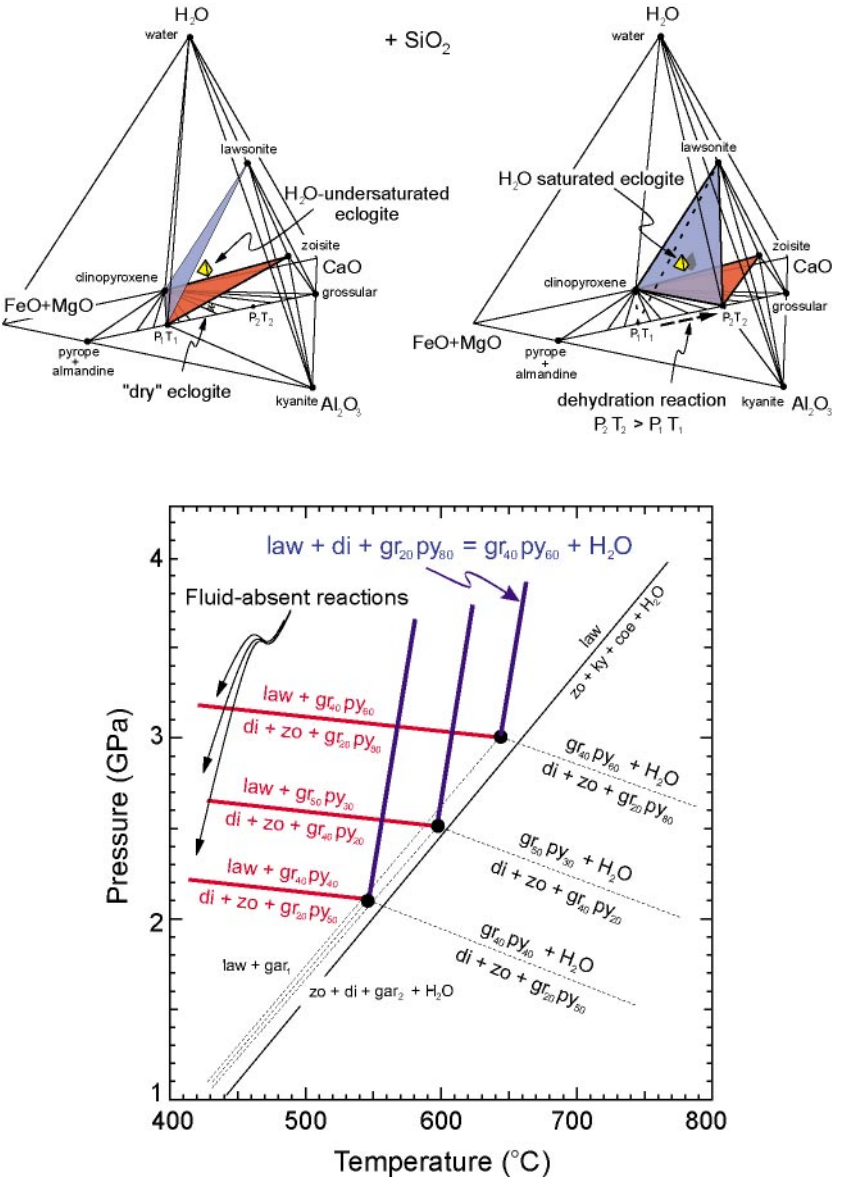

Figure 6 Schematic chemographies and P-T phase diagram for the system CFMASH that show how H_2O-saturated assemblages form from H_2O-undersaturated assemblages via continuous reactions involving garnet as a solid solution. Univariant reactions in *red* stand for phase transformations related to displacement of phase boundary in *red* in chemography (*a*) and (*b*). gr: grossular; py: pyrope; di: diopside; zo: zoisite. $gr_{50}py_{30}$ stands for a ternary garnet having 50 mol% grossular component, 30 mol% pyrope, 20 mol% almandine. After Poli & Schmidt 1997. See text for details.

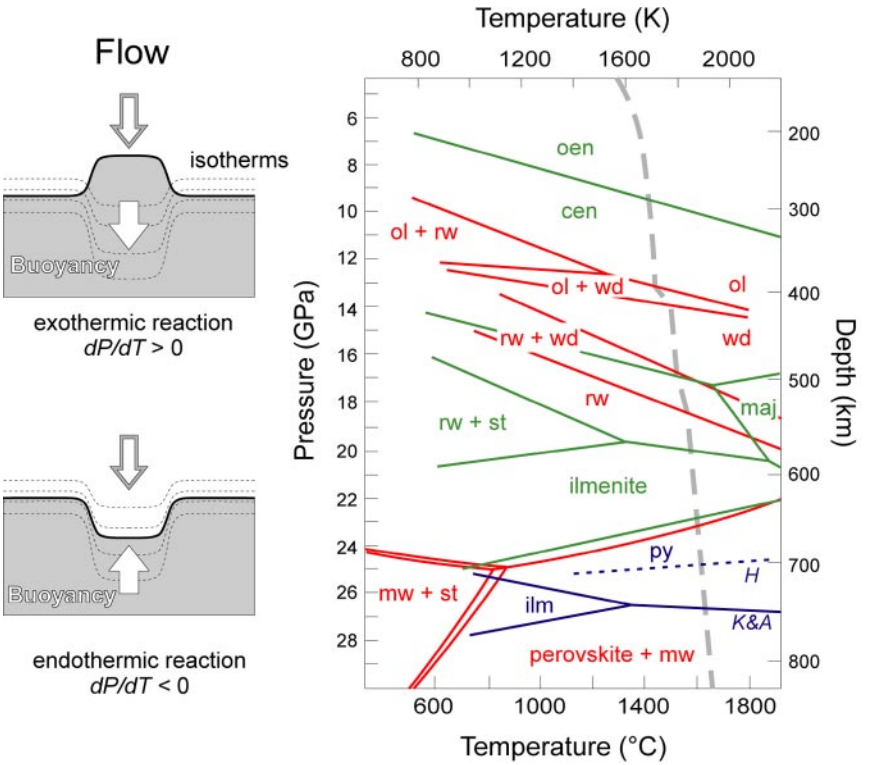

Figure 11 Effect of Clapeyron slope on the buoyancy forces. *Red lines* on the P-T diagram on the right side represent phase fields for $(Mg_{0.89},Fe_{0.11})_2SiO_4$ after Akaogi et al. 1998; *green lines* are for the system $MgSiO_3$, from Fei & Bertka 1999. *Blue lines* are for the system $Mg_3Al_2Si_3O_{12}$, H is from Hirose 2001, K & A is from Kubo & Akaogi 2000. The *dashed line* represents a mantle adiabat (Ito & Sato 1992).

Annual Review of Earth and Planetary Sciences
Volume 30, 2002

CONTENTS